show significant linkage between *H-2* and major autoimmune traits examined. These results indicate a minor influence of dimorphism – $H\text{-}2^k$ (MRL/lpr haplotype) or $H\text{-}2^b$ (B6/lpr haplotype) – on the development of autoimmune diseases. These, in turn, suggest a major contribution of the non-*H-2* loci; however, a sufficient set of such susceptibility loci remains undermined. MBN2 mice develop autoimmune disorders under varied genetic conditions, wherein a number of minor susceptibility loci influence the onset of autoimmune diseases, probably, in an interactive fashion of multiple loci. It should be considered that a conventional method for genome-wide screening, as performed in this study, limits the sensitivity for minor and/or interactive linkage loci.

A majority of human autoimmune diseases occur in a female-predominant fashion [1]. This study suggests the presence of a male-specific mechanism underlying the SrD in autoimmune diseases. It is further suggested that this mechanism is achieved by some autosomal gene functions controlled under undetermined male-specific conditions associated with sex-related hormones and/or the Y chromosome. Further understanding of the molecular details of this mechanism will provide a clue with regard to the general therapeutic approach for human autoimmune diseases.

Materials and methods

Mice

MRL/lpr and B6/lpr mice were purchased from the Charles River Japan, Yokohama, Japan. These mice were bred under specific pathogen-free condition in the Integrated Center of Science in Ehime University, Toon, Japan, or the Institute for Animal Experimentation Tohoku University, Sendai, Japan. MBF1 and the backcross MBN2 were prepared and housed in these centers. In all animal experiments in this study, we observed the Ehime University and Tohoku University guidelines for animal experimentation.

Histological evaluation of GN

At 19–20 weeks of age, mice were killed under ether anesthesia. After sampling blood for serum isolation, the removed kidneys were fixed with 10% formalin in 0.01 M phosphate buffer, pH 7.2, and embedded in paraffin. Tissue sections were stained with periodic acid-Schiff. GN was microscopically graded under the criteria for an increase in a cellular or matrix component in the glomerulus (Supporting Information Fig. 1). An increase in a cellular component was graded on a scale of 0–3: 0, normal cellularity; 1, slight cellular proliferation; 2, enlargement of glomerulus with remarkable cellular proliferation; and 3, crescent formation. An increase in a matrix component was graded on a scale of 0–3: 0, normal; 1, slight mesangial increase; 2, lobulation or segmental sclerosis; and 3, global sclerosis. No less than 30 glomeruli for an individual were examined, then an individual GN index was defined by $\log_{10}$ [(a mean of cellular grades) + (a mean of matrix grades)].

Measurement of ANA

ANA titer was measured with the indirect immunofluorescence (IF) method applying to nuclear samples prepared from a normal mouse liver as described previously [49]. Nuclear samples were incubated with serum dilution and antibody of FITC-conjugated anti-mouse IgG, γ chain specific (Zymed, South San Francisco, CA) or anti-mouse IgM, μ chain specific (Zymed). ANA titer was determined by a fluorescence detection of nuclear signal with following standards: 0, no staining with 1:100 serum dilution; 1, faintly stained with 1:100 serum dilution; 2, clearly stained with1:100 serum dilution; 3, stained with 1:1000 serum dilution; 4, stained with 1:10000 serum dilution; 5, stained with 1:30 000 serum dilution; 6, stained with1:90 000 serum dilution.

Mapping of autoimmune-associated loci

The genotypes of MBN2 mice were determined using mouse microsatellite markers whose genetic positions are determined by the Mouse Genome Informatics (MGI), The Jackson laboratory. PCR was performed under the following conditions: 94°C for 2 min, 35 cycles of 94°C for 30 s, 55°C for 30 s, 72°C for 30 s, and a final extension at 72°C for 5 min. PCR products were visualized on 4% agarose gels by staining with ethidium bromide after electrophoresis.

In genome-wide screenings, we determined 117 microsatellite genotypes of randomly selected 95 MBN2 mice (Supporting Information Fig. 2). These markers provide a full coverage of mouse autosomes with an average of 12.9 cM apart (maximum distance is 23 cM). Both X chromosomes of every female MBN2 mouse were derived from MRL/lpr; therefore, we did not test X chromosome in this study. In QTL analysis, we determined the genotypes of another 253 MBN_2 mice (a total of 348 mice) on candidate chromosomes.

Statistical analysis

We adopted $\log_{10}$-transformed values of spleen weights (mg) and GN indexes to obtain normal distributions. In association studies, $p<0.0034$ and $p<0.0001$ were accepted as suggestive and significant linkage, respectively [50]. A QTL analysis was performed using Windows QTL Cartographer (V2.5) software with each autoimmune traits in MBN_2 mice [51]. Interval mapping program was adopted and walk-speed was 2 cM. A significant and suggestive threshold level of LOD score was determined by the permutation test (1000 permutation with $\alpha=0.01$ or 0.05, respectively). To evaluate interaction of two QTL, we used the R/qtl program available at http://www.biostat.jhsph.edu/~kbroman/qtl [26]. Significant threshold level was determined by the permutation test installed in this program (100 permutations, $\alpha=0.05$). Spearman's rank correlation, Student's *t*-test, and one-way analysis of variance (ANOVA) were also used in the present study. $p<0.05$ was estimated as significant.

Acknowledgements: The authors thank Dr. Norio Sugawara for helps in statistical analyses, Dr. Tatsuro Misu for critical advise in manuscript preparation, Ms. Fumiko Date and Ms. Miho Terada for technical assistances, and Mrs. Noriko Fujisawa for secretarial assistance. This work is supported by Grants-in-Aid for Scientific Research from the Ministry of Education, Science, Sports, and Culture of Japan to M.O. (No.16390113, 19390108, and 19659096).

References

1 **Whitacre, C. C.**, Sex differences in autoimmune disease. *Nat. Immunol.* 2001. **2**: 777–780.

2 **Raveche, E. S., Tjio, J. H., Boegel, W. and Steinberg, A. D.**, Studies of the effects of sex hormones on autosomal and X-linked genetic control of induced and spontaneous antibody production. *Arthritis Rheum.* 1979. **22**: 1177–1187.

3 **Carlsten, H, Nilsson, N, Jonsson, R, Backman, K, Holmdahl, R. and Tarkowski, A.**, Estrogen accelerates immune complex glomerulonephritis but ameliorates T cell-mediated vasculitis and sialadenitis in autoimmune MRL lpr/lpr mice. *Cell. Immunol.* 1992. **144**: 190–202

4 **Steinberg, A. D., Melez, K. A., Raveche, E. S., Reeves, J. P., Boegel, W. A., Smathers, P. A., Taurog, J. D. *et al.***, Approach to the study of the role of sex hormones in autoimmunity. *Arthritis Rheum.* 1979. **22**: 1170–1176.

5 **Sthoeger, Z. M., Zinger, H. and Mozes, E.**, Beneficial effects of the anti-oestrogen tamoxifen on systemic lupus erythematosus of (NZB x NZW)F1 female mice are associated with specific reduction of IgG3 autoantibodies. *Ann. Rheum. Dis.* 2003. **62**: 341–346.

6 **Apelgren, L. D., Bailey, D. L., Fouts, R. L., Short, L., Bryan, N., Evans, G. F., Sandusky, G. E. *et al.***, The effect of a selective estrogen receptor modulator on the progression of spontaneous autoimmune disease in MRL/lpr/lpr mice. *Cell. Immunol.* 1996. **173**: 55–63.

7 **Roubinian, J. R., Papoian, R. and Talal, N.**, Androgenic hormones modulate autoantibody responses and improve survival in murine lupus. *J. Clin. Invest.* 1977. **59**: 1066–1070.

8 **Roubinian, J. R., Talal, N., Greenspan, J. S., Goodman, J. R. and Siiteri, P. K.**, Effect of castration and sex hormone treatment on survival, anti-nucleic acid antibodies, and glomerulonephritis in NZB/NZW F1 mice. *J. Exp. Med.* 1978. **147**: 1568–1583.

9 **Liu, Z. H., Cheng, Z. H., Gong, R. J., Liu, H., Liu, D. and Li, L. S.**, Sex differences in estrogen receptor gene polymorphism and its association with lupus nephritis in Chinese. *Nephron* 2002. **90**: 174–180.

10 **Ushiyama, T., Mori, K., Inoue, K., Huang, J., Nishioka, J. and Hukuda, S.**, Association of oestrogen receptor gene polymorphisms with age at onset of rheumatoid arthritis. *Ann. Rheum. Dis.* 1999. **58**: 7–10.

11 **Takagi, H., Ishiguro, N., Iwata, H. and Kanamono, T.**, Genetic association between rheumatoid arthritis and estrogen receptor microsatellite polymorphism. *J. Rheumatol.* 2000. **27**: 1638–1642.

12 **Araneo, B. A., Dowell, T., Diegel, M. and Daynes, R. A.**, Dihydrotestosterone exerts a depressive influence on the production of interleukin-4 (IL-4), IL-5, and gamma-interferon, but not IL-2 by activated murine T cells. *Blood* 1991. **78**: 688–699.

13 **Bengtsson, A. K., Ryan, E. J., Giordano, D., Magaletti, D. M. and Clark, E. A.**, 17{beta}-Estradiol (E2) modulates cytokine and chemokine expression in human monocyte-derived dendritic cells. *Blood* 2004. **104**: 1404–1410.

14 **Zinman, B., Kabiawu, S. I., Moross, T., Berg, J., Lupmanis, A., Markovic, V. and Gardner, H. A.**, Endocrine, cytogenetic and psychometric features of patients with X-isochromosome 46, X, i(Xq) Turner's syndrome: a preliminary study in nine patients. *Clin. Invest. Med.* 1984. **7**: 135–141.

15 **Fleming, S., Cowell, C., Bailey, J. and Burrow, G. N.**, Hashimoto's disease in Turner's syndrome. *Clin. Invest. Med.* 1988. **11**: 243–246.

16 **Invernizzi, P., Miozzo, M., Selmi, C., Persani, L., Battezzati, P. M., Zuin, M., Lucchi, S. *et al.***, X chromosome monosomy: a common mechanism for autoimmune diseases. *J. Immunol.* 2005. **175**: 575–578.

17 **Morse, H. C., 3rd, Davidson, W. F., Yetter, R. A., Murphy, E. D., Roths, J. B. and Coffman, R. L.**, Abnormalities induced by the mutant gene lpr: expansion of a unique lymphocyte subset. *J. Immunol.* 1982. **129**: 2612–2615.

18 **Watanabe-Fukunaga, R., Brannan, C. I., Copeland, N. G., Jenkins, N. A. and Nagata, S.**, Lymphoproliferation disorder in mice explained by defects in Fas antigen that mediates apoptosis. *Nature* 1992. **356**: 314–317.

19 **Izui, S., Kelley, V. E., Masuda, K., Yoshida, H., Roths, J. B. and Murphy, E. D.**, Induction of various autoantibodies by mutant gene lpr in several strains of mice. *J. Immunol.* 1984. **133**: 227–233.

20 **Theofilopoulos, A. N. and Dixon, F. J.**, Murine models of systemic lupus erythematosus. *Adv. Immunol.* 1985. **37**: 269–390.

21 **Nose, M., Nishimura, M. and Kyogoku, M.**, Analysis of granulomatous arteritis in MRL/Mp autoimmune disease mice bearing lymphoproliferative genes. The use of mouse genetics to dissociate the development of arteritis and glomerulonephritis. *Am. J. Pathol.* 1989. **135**: 271–280.

22 **Andrews, B. S., Eisenberg, R. A., Theofilopoulos, A. N., Izui, S., Wilson, C. B., McConahey, P. J., Murphy, E. D. *et al.***, Spontaneous murine lupus-like syndromes. Clinical and immunopathological manifestations in several strains. *J. Exp. Med.* 1978. **148**: 1198–1215.

23 **Wang, Y., Nose, M., Kamoto, T., Nishimura, M. and Hiai, H.**, Host modifier genes affect mouse autoimmunity induced by the lpr gene. *Am. J. Pathol.* 1997. **151**: 1791–1798.

24 **Gu, L., Weinreb, A., Wang, X. P., Zack, D. J., Qiao, J. H., Weisbart, R. and Lusis, A. J.**, Genetic determinants of autoimmune disease and coronary vasculitis in the MRL/lpr/lpr mouse model of systemic lupus erythematosus. *J. Immunol.* 1998. **161**: 6999–7006.

25 **Zhang, M. C., Misu, N., Furukawa, H., Watanabe, Y., Terada, M., Komori, H., Miyazaki, T. *et al.***, An epistatic effect of the female specific loci on the development of autoimmune vasculitis and antinuclear autoantibody in murine lupus. *Ann. Rheum. Dis.* 2006. **65**: 495–500.

26 **Broman, K. W., Wu, H., Sen, S. and Churchill, G. A.**, R/qtl: QTL mapping in experimental crosses. *Bioinformatics* 2003. **19**: 889–890.

27 **van den Ouweland, J. M., Lemkes, H. H., Ruitenbeek, W., Sandkuijl, L. A., de Vijlder, M. F., Struyvenberg, P. A., van de Kamp, J. J. *et al.***, Mutation in mitochondrial tRNA(Leu)(UUR) gene in a large pedigree with maternally transmitted type II diabetes mellitus and deafness. *Nat. Genet.*. **1**: 368–371.

28 **Harding, A. E., Sweeney, M. G., Miller, D. H., Mumford, C. J., Kellar-Wood, H., Menard, D., McDonald, W. I. *et al.***, Occurrence of a multiple sclerosis-like illness in women who have a Leber's hereditary optic neuropathy mitochondrial DNA mutation. *Brain* 1992. **115**: 979–989.

29 **Burch, P. R.**, Klinefelter's syndrome, dizygotic twinning and diabetes mellitus. *Nature* 1969. **221**: 175–177.

30 **Ortiz-Neu, C. and LeRoy, E. C.**, The coincidence of Klinefelter's syndrome and systemic lupus erythematosus. *Arthritis Rheum.* 1969. **12**: 241–346.

31 **Teuscher, C., Noubade, R., Spach, K., McElvany, B., Bunn, J. Y., Fillmore, P. D., Zachary, J. F. *et al.***, Evidence that the Y chromosome influences autoimmune disease in male and female mice. *Proc. Natl. Acad. Sci. USA* 2006. **103**: 8024–8029.

32 **Vidal, S., Kono, D. H. and Theofilopoulos, A. N.**, Loci predisposing to autoimmunity in MRL-Fas^{lpr} and C57BL/6-Fas^{lpr} mice. *J. Clin. Invest.* 1998. **101**: 696–702.

33 **Kono, D. H., Burlingame, R. W., Owens, D. G., Kuramochi, A., Balderas, R. S., Balomenos, D. and Theofilopoulos, A. N.**, Lupus susceptibility loci in New Zealand mice. *Proc. Natl. Acad. Sci. USA* 1994. **91**: 10168–10172.

34 **Morel, L., Rudofsky, U. H., Longmate, J. A., Schiffenbauer, J. and Wakeland, E. K.**, Polygenic control of susceptibility to murine systemic lupus erythematosus. *Immunity* 1994. **1**: 219–229.

35 **Miyazaki, T., Ono, M., Qu, W. M., Zhang, M. C., Mori, S., Nakatsuru, S., Nakamura, Y. *et al.***, Implication of allelic polymorphism of osteopontin in the development of lupus nephritis in MRL/lpr mice. *Eur. J. Immunol.* 2005. **35**: 1510–1520.

36 **Morel, L., Tian, X. H., Croker, B. P. and Wakeland, E. K.**, Epistatic modifiers of autoimmunity in a murine model of lupus nephritis. *Immunity* 1999. **11**: 131–139.

37 Drake, C. G., Babcock, S. K., Palmer, E. and Kotzin, B. L., Genetic analysis of the NZB contribution to lupus-like autoimmune disease in (NZB x NZW)F1 mice. *Proc. Natl. Acad. Sci. USA* 1994. 91: 4062–4066.

38 Watson, M. L., Rao, J. K., Gilkeson, G. S., Ruiz, P., Eicher, E. M., Pisetsky, D. S., Matsuzawa, A. *et al.*, Genetic analysis of MRL/lpr mice: relationship of the Fas apoptosis gene to disease manifestations and renal disease-modifying loci. *J. Exp. Med.* 1992. 176: 1645–1656.

39 Qu, W. M., Miyazaki, T., Terada, M., Lu, L. M., Nishihara, M., Yamada, A., Mori, S. *et al.*, Genetic dissection of vasculitis in MRL/lpr lupus mice: a novel susceptibility locus involving the *CD72*^{c} allele. *Eur. J. Immunol.* 2000. 30: 2027–2037.

40 Jury, E. C., Kabouridis, P. S., Abba, A., Mageed, R. A. and Isenberg, D. A., Increased ubiquitination and reduced expression of LCK in T lymphocytes from patients with systemic lupus erythematosus. *Arthritis Rheum.* 2003. 48: 1343–1354.

41 Bowness, P., Davies, K. A., Norsworthy, P. J., Athanassiou, P., Taylor-Wiedeman, J., Borysiewicz, L. K., Meyer, P. A. *et al.*, Hereditary C1q deficiency and systemic lupus erythematosus. *QJM* 1994. 87: 455–464.

42 Botto, M., Dell'Agnola, C., Bygrave, A. E., Thompson, E. M., Cook, H. T., Petry, F., Loos, M. *et al.*, Homozygous C1q deficiency causes glomerulonephritis associated with multiple apoptotic bodies. *Nat. Genet.* 1998. 19: 56–59.

43 Miura-Shimura, Y., Nakamura, K., Ohtsuji, M., Tomita, H., Jiang, Y., Abe, M., Zhang, D. *et al.*, C1q regulatory region polymorphism down-regulating murine c1q protein levels with linkage to lupus nephritis. *J. Immunol.* 2002. 169: 1334–1339.

44 Hall, A. V., Parbtani, A., Clark, W. F., Spanner, E., Keeney, M., Chin-Yee, I., Philbrick, D. J. *et al.*, Abrogation of MRL/lpr lupus nephritis by dietary flaxseed. *Am. J. Kidney Dis.* 1993. 22: 326–332.

45 Tetta, C., Bussolino, F., Modena, V., Montrucchio, G., Segoloni, G., Pescarmona, G. and Camussi, G., Release of platelet-activating factor in systemic lupus erythematosus. *Int. Arch. Allergy Appl. Immunol.* 1990. 91: 244–256.

46 Mary, C., Laporte, C., Parzy, D., Santiago, M. L., Stefani, F., Lajaunias, F., Parkhouse, R. M. *et al.*, Dysregulated expression of the *Cd22* gene as a result of a short interspersed nucleotide element insertion in *Cd22*^{a} lupus-prone mice. *J. Immunol.* 2000. 165: 2987–2996.

47 Dorner, T., Kaufmann, J., Wegener, W. A., Teoh, N., Goldenberg, D. M. and Burmester, G. R., Initial clinical trial of epratuzumab (humanized anti-CD22 antibody) for immunotherapy of systemic lupus erythématosus. *Arthritis Res. Ther.* 2006. 8: R74.

48 Kikuchi, S., Fossati-Jimack, L., Moll, T., Amano, H., Amano, E., Ida, A., Ibnou-Zekri, N. *et al.*, Differential role of three major New Zealand Black-derived loci linked with Yaa-induced murine lupus nephritis. *J. Immunol.* 2005. 174: 1111–1117.

49 Komori, H., Furukawa, H., Mori, S., Ito, M.R., Terada, M., Zhang, M.C., Ishii, N. *et al.*, A signal adaptor SLAM-associated protein regulates spontaneous autoimmunity and Fas-dependent lymphoproliferation in MRL-*Fas*^{lpr} lupus mice. *J. Immunol.* 2006. 176: 395–400.

50 Lander, E. and Kruglyak, L., Genetic dissection of complex traits: guidelines for interpreting and reporting linkage results. *Nat. Genet.* 1995. 11: 241–247.

51 Zeng, Z. B., Precision mapping of quantitative trait loci. *Genetics* 1994. 136: 1457–1468.

Association of Gankyrin Protein Expression with Early Clinical Stages and Insulin-Like Growth Factor-Binding Protein 5 Expression in Human Hepatocellular Carcinoma

Atsushi Umemura,[1,2] Yoshito Itoh,[2] Katsuhiko Itoh,[1] Kanji Yamaguchi,[2] Tomoki Nakajima,[2] Hiroaki Higashitsuji,[1] Hitoshi Onoue,[3] Manabu Fukumoto,[4] Takeshi Okanoue,[2] and Jun Fujita[1]

Gankyrin (also known as PSMD10) is a liver oncoprotein that interacts with multiple proteins including MDM2 and accelerates degradation of the tumor suppressors p53 and Rb. We produced a monoclonal anti-gankyrin antibody and immunohistochemically assessed the clinicopathological significance of gankyrin overexpression in 43 specimens of human hepatocellular carcinoma (HCC). Specific cytoplasmic staining for gankyrin was observed in 62.8% (27/43) of HCCs, which was significantly associated with low TNM stage ($P = 0.004$), no capsular invasion ($P = 0.018$), no portal venous invasion ($P = 0.008$), and no intrahepatic metastasis ($P = 0.012$). The cumulative survival rate of patients with gankyrin-positive HCC was significantly higher than that with gankyrin-negative HCC ($P = 0.037$). p53 and MDM2 were positively stained by antibodies in 30.2% and 23.3%, respectively, of HCCs, but neither was inversely associated with gankyrin expression. In the Huh-7 human HCC cell line, overexpression of gankyrin up-regulated expression of insulin-like growth factor binding protein 5 (IGFBP-5), whereas suppression of gankyrin expression by siRNA down-regulated it. Supression of IGFBP-5 expression inhibited proliferation of Huh-7 cells as well as U-2 OS osteosarcoma cells. In HCC specimens, positive staining for IGFBP-5 was observed by immunohistochemistry in 41.9% (18/43), and the level of expression was significantly correlated with that of gankyrin (*rho* = 0.629, $P < 0.001$). *Conclusion:* These results suggest that gankyrin plays an oncogenic role(s) mainly at the early stages of human hepatocarcinogenesis, and that IGFBP-5 inducible by gankyrin overexpression may be involved in it. (HEPATOLOGY 2008;47:493-502.)

Liver cancer is the sixth most common cancer worldwide (626,000 or 5.7% of new cancer cases) and the third most common cause of death from cancer (598,000) in 2002.[1] Eighty-two percent of cases are in developing countries, and the areas of high incidence are sub-Saharan Africa, eastern and southeastern Asia, and Melanesia. Histologically, more than 90% of the primary liver cancers are hepatocellular carcinomas (HCCs). Although there are several modalities of treatment for HCC, most patients present with unresectable tumors, and nonsurgical treatments are minimally effective at best.[2,3] Even for those patients who undergo surgical resection, the recurrence rate is very high and the prognosis is poor.[2,4-6] It is therefore important to clarify the mechanisms of human hepatocarcinogenesis and identify molecular targets to develop novel diagnostic, therapeutic, and preventive strategies.

By constructing subtracted complementary DNA (cDNA) libraries, we have previously identified 19 genes overexpressed in HCCs including 2 novel genes.[7,8] One of them was named gankyrin (gann-ankyrin repeat pro-

Abbreviations: 3A6C2, mouse monoclonal anti-gankyrin antibody; cDNA, complementary DNA; HCC, hepatocellular carcinoma; IGF, insulinlike growth factor; IGFBP-5, insulin-like growth factor-binding protein 5; MDM2, mouse double minute 2; mRNA, messenger RNA; RT-PCR, reverse transcription polymerase chain reaction; siRNA, short interfering RNA; TNM, tumor-node-metastasis.

From the [1]Department of Clinical Molecular Biology, Graduate School of Medicine, Kyoto University, Kyoto, Japan; the [2]Molecular Gastroenterology and Hepatology, Graduate School of Medical Science, Kyoto Prefectural University of Medicine, Kyoto, Japan; the [3]Department of Nutritional Science, Faculty of Health and Welfare, Seinun Jo Gakuin University, Kitakyushu, Japan; and the [4]Department of Pathology, Institute of Development, Aging, and Cancer, Tohoku University, Sendai, Japan

Received May 21, 2007; accepted September 3, 2007.

Supported by Grants-in aid from the Ministry of Education, Culture, Sports, Science, and Technology of Japan and the Japan Society for the Promotion of Science.

Address reprint requests to: Jun Fujita, Department of Clinical Molecular Biology, Graduate School of Medicine, Kyoto University, 54 Shogoin Kawaharacho, Sakyo-ku, Kyoto 606-8507, Japan. E-mail: jfujita@virus.kyoto-u.ac.jp; fax: (81) 75-751-4977.

Published online in Wiley InterScience (www.interscience.wiley.com).

DOI 10.1002/hep.22027

Potential conflict of interest: Nothing to report.

tein; "gann" in Japanese means cancer).[9] Gankyrin (also called PSMD10) consists of 7 ankyrin repeats, and its messenger RNA (mRNA) was overexpressed in 34 of 34 HCCs analyzed.[9,10] Independently, gankyrin was isolated as the p28 component or the interactor of the S6b subunit of the 19S regulator of the 26S proteasome.[11,12] The ankyrin repeat is the functional domain involved in protein–protein interactions, and gankyrin has been shown to interact with multiple proteins in addition to S6b. Gankyrin binds to retinoblastoma protein (Rb) and cyclin-dependent kinase (Cdk4), and accelerates phosphorylation and degradation of Rb, which results in release of the E2F transcription factor to activate DNA synthesis genes.[9,13] Gankyrin seems to play a role in cell cycle progression in noncancerous cells as well. Overexpression of gankyrin shortens population doubling time of NIH/3T3 mouse fibroblasts,[9] and its up-regulation correlates with cell cycle progression in normal rat primary hepatocytes, oval cells, and human hepatocytes.[14,15]

Overexpression of gankyrin confers tumorigenicity to NIH/3T3 cells and inhibits apoptosis in cultured human tumor cells exposed to chemotherapeutic agents.[10] The anti-apoptotic activity is attributable, at least partly, to increased degradation of p53, resulting in the reduced transcription of the p53-dependent proapoptotic genes.[16] Gankyrin binds to the E3 ubiquitin ligase MDM2 *in vitro* and *in vivo*, which increases p53–MDM2 association, thereby facilitating the ubiquitination and subsequent proteasomal degradation of p53 by MDM2. Gankyrin also controls MDM2 auto-ubiquitination and degradation, especially in the absence of p53.[16]

We produced a mouse monoclonal antibody against human gankyrin and assessed the expression of gankyrin protein in surgically resected HCC specimens by immunohistochemistry. Correlation of gankyrin positivity with clinicopathological findings and expression of p53 and MDM2 in HCC was analyzed. Furthermore, we demonstrated that expression of insulin-like growth factor-binding protein 5 (IGFBP-5) is inducible by overexpression of gankyrin in HCCs.

Patients and Methods

Patients and Specimens. HCC tissues and their corresponding noncancerous liver tissues were obtained from 43 and 32 patients, respectively, who had undergone curative hepatectomy at the University Hospital of Kyoto Prefectural University of Medicine between 1992 and 2000. The specimens used were routinely processed, formalin-fixed, and paraffin-embedded. After hematoxylin-eosin staining, all samples were diagnosed as HCC and the tumor-node-metastasis (TNM) classification was made according to the fourth edition of the general rules for the clinical and pathological study of primary liver cancer proposed by the Liver Cancer Study Group of Japan.[17] The demographic profiles of the patients are summarized in Table 1. For western blot analysis, HCCs and noncancerous liver tissues were obtained from 3 patients undergoing liver transplantation at the University Hospital of Kyoto Prefectural University of Medicine between 2004 and 2006. No donor organs were obtained from executed prisoners or other institutionalized persons. The study protocol conformed to the ethical guidelines of the 1975 Declaration of Helsinki and was approved by the institutional review boards. Written informed consents were obtained from all patients for subsequent use of their resected tissues.

Table 1. Patient and Tumor Characteristics

Characteristic	Number (Percentage)
Number of patients	43
Sex distribution	
Male	27 (62.8%)
Female	16 (37.2%)
Age (years)	25-78, median 65
Virus marker	
HBV(+)/HCV(−)	6 (14.0%)
HBV(−)/HCV(+)	28 (65.0%)
HBV(+)/HCV(+)	3 (7.0%)
HBV(−)/HCV(−)	6 (14.0%)
AFP(ng/mL)	3.5-39999, median 90
Tumor size (cm)	1.6-17.0, median 4.0
Liver cirrhosis	
Yes	29 (67.5%)
No	14 (32.5%)
Chronic hepatitis	13 (30.2%)
Normal	1 (2.3%)
TNM stage	
I	4 (9.3%)
II	22 (51.1%)
III	8 (18.6%)
IV	9 (21.0%)
Histological differentiation	
Well	12 (27.9%)
Moderate	25 (58.1%)
Poor	6 (14.0%)
Capsular formation	
Yes	36 (83.7%)
No	7 (16.3%)
Capsular invasion	
Yes	14 (32.6%)
No	29 (67.4%)
Portal venous invasion	
Yes	9 (20.9%)
No	34 (79.1%)
Intrahepatic metastasis	
Yes	16 (37.2%)
No	27 (62.8%)

Abbreviations: HCV(+), anti-hepatitis C virus antibody positive; HBV(+), hepatitis B surface antigen positive; (−), negative; AFP, serum alpha-fetoprotein.

Cell Culture and Transfection. Huh-7 human HCC cells, U-2 OS human osteosarcoma cells, 293T human embryonic kidney cells, mouse lymph node cells, and P3X63Ag8U.1 mouse myeloma cells were cultured in Dulbecco's modified Eagle's medium (Gibco BRL Life Technologies, NY) supplemented with 10% fetal bovine serum as described.[16] To assess viable cell numbers, we used the Dojindo Cell Counting Kit-8 (CCK8 kit, Dojindo Laboratories, Kumamoto, Japan) according to the manufacturer's instructions.

The 293T, Huh-7, and U-2 OS cells were transfected with plasmid DNA by using the calcium phosphate method or FuGENE 6 Transfection Reagent (Roche Diagnostics, Mannheim, Germany) as described.[16] Short interfering RNA (siRNA) were transfected at a final concentration of 25 nM by using siPORT NeoFX Transfection Agent (Ambion, Austin, TX) following the manufacturer's instructions. Twenty-four hours after transfection, the medium was replaced with fresh medium containing fetal bovine serum, and the culture was continued for another 24 or 48 hours. Then, the cells were harvested for analysis. All transfection assays were repeated at least 3 times.

Plasmids and siRNA. Human wild-type gankyrin cDNAs, full coding sequence and deletion mutants, were cloned into the mammalian expression vector pMKIT-NEO and expressed as hemagglutinin (HA)-tagged proteins (Fig. 1A). Full-length gankyrin was expressed without a tag as well. To obtain recombinant human gankyrin protein, the full-length cDNA was cloned into an expression vector derived from pET28 (Novagen, EMD Biosciences Inc., San Diego, CA) and expressed as hexahistidine-tagged protein.

To down-regulate gene expression, Silencer Predesigned siRNAs for gankyrin (Ambion) and Stealth Select iRNA: for IGFBP-5 (Invitrogen, Tokyo, Japan), were used together with respective control RNAs.

Antibodies. To obtain monoclonal antibodies against human gankyrin, recombinant (His)6-gankyrin protein was used as an immunogen. It was dissolved in phosphate-buffered saline (1 mg/mL) and emulsified with an equal volume of Freund's complete adjuvant (Difco, Becton-Dickinson, Franklin Lakes, NJ). Two female BALB/c mice were injected with the emulsion (50 μL/mouse) in the footpad. Two weeks after immunization, the inguinal lymph node cells (4×10^7 cells) were fused with P3X63Ag8U.1 myeloma cells (1×10^7) using polyethylene glycol 1500 (Roche Diagnostics). Fused cells were cultured in 96-well plates at 2×10^5 cell/well. The supernatants were assayed for the anti-gankyrin antibody titer by an enzyme-linked immunosorbent assay using recombinant His-tagged, glutathione-S-transferase (GST)-tagged, and nontagged gankyrin proteins. Selected relevant hybridomas were cloned by the limiting dilution method, and the isotypes of secreted monoclonal antibodies were determined by the IsoStrip kit (Roche Diagnostics) following the manufacturer's instructions. Finally, an IgG2b kappa monoclonal antibody that showed the highest affinity for gankyrin was obtained and named 3A6C2.

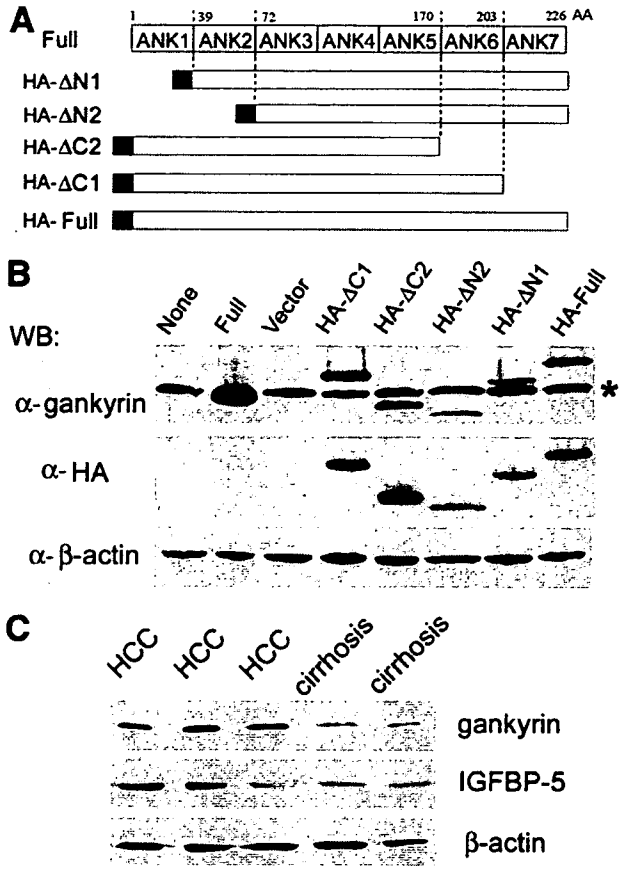

Fig. 1. Recognition of gankyrin protein by the monoclonal antibody. (A) Structures of wild-type gankyrin (Full) and its deletion mutants. Numbers on top, N- and C-terminal amino-acid residues. ANK, ankyrin repeat. Black bars, HA tags. (B) Specificity of the antibody. 293T cells were transfected with plasmids expressing the indicated proteins. Cell lysates were analyzed by western blotting (WB) using the anti-gankyrin monoclonal antibody (3A6C2), anti-HA antibody, and anti-β-actin antibody. *Mobility of the endogenous gankyrin. Representative results of 3 repeated experiments are shown. (C) Detection of gankyrin protein in tissues. Lysates were made from hepatocellular carcinoma (HCC, n = 3) and cirrhotic liver tissues (n = 2), and analyzed by WB using antibodies for indicated proteins. HA, hemagglutinin.

For western blot analysis, mouse monoclonal anti-gankyrin antibody (3A6C2), goat polyclonal anti-IGFBP-5 antibody (R&D Systems Inc., Minneapolis, MN), mouse monoclonal anti-HA antibody (12CA5, Roche Diagnostics), and mouse monoclonal anti-β-actin antibody (Chemicon International, Temecula, CA) were

used. Horseradish peroxidase–conjugated secondary antibodies against mouse or goat immunoglobulins were obtained from DAKO (Kyoto, Japan).

For immunohistochemistry, mouse monoclonal anti-gankyrin (3A6C2), anti-MDM2 (Ab-4, Oncogene research products, Boston, MA), and anti-p53 (DO-7, DAKO) antibodies, rabbit polyclonal anti-IGFBP-5 antibody (GroPep, Thebarton, Australia), and horseradish peroxidase–conjugated secondary antibodies against mouse or rabbit immunoglobulins (DAKO) were used.

Analysis of Gene Expression. Extraction of RNA, preparation of cell and tissue lysates, and western blot analysis were performed as described.[9] Real-time reverse transcription polymerase chain reaction (RT-PCR) analysis was performed using ABI PRISM 7900 (Applied Biosystems, Foster City, CA) and a 1-step QuantiTect RT-PCR Kit (Qiagen, Cowley, UK) according to the manufacturer's instructions. PCR conditions were 50°C for 30 minutes and 95°C for 15 minutes, followed by 45 cycles of 95°C for 15 seconds, 55°C for 30 seconds, and 72°C for 45 seconds. Specific PCR amplification products were detected by SYBR Green. Transcripts of β-actin were quantified as control. Primer sequences used were as follows: IGFBP-5, AAGAAGCTGACCCAGTCCAA and GAATCCTTTGCGGTCACAAT; gankyrin, GCAACTTGGAGTGCCAGTGAA and TCACTTGAGCACCTTTTCCCA; β-actin, CTACGTCGCCCTGGACTTCGAGC and GATGGAGCCGCCGATCCACACGG.

The immunohistochemical staining was performed on 4-μm-thick paraffin sections of tissues fixed in buffered formalin. The sections were pretreated with 10 mM citrate buffer (pH 6.1) in a microwave oven for 5 minutes. Endogenous peroxidase activity was blocked with 0.3 % H_2O_2 for 10 minutes. The sections were incubated with 10% fetal bovine serum for 30 minutes to reduce nonspecific binding, followed by incubation with the primary antibody at 4°C overnight. They were subsequently incubated with horseradish peroxidase–conjugated anti-mouse or rabbit immunoglobulin antibody for 30 minutes. The enzymatic reaction was developed in a freshly prepared solution of 3,3′-diaminobenzidine tetrahydrochloride using DAKO Liquid DAB Substrate-Chromogen Solution for 10 minutes at room temperature. The sections were then counterstained with hematoxylin. The staining pattern, the distribution of the immunostaining in each tissue, and the intensity of the staining were studied in detail. Negative controls were conducted by substituting normal sera of each animal for the primary antibodies. When immunoreactivities were heterogenously observed, cases with moderate or strong staining of nucleus or cytoplasm in more than 5% of the cells were considered positive. To analyze the correlation of the expression levels of gankyrin and IGFBP-5, the staining intensity was expressed as 0 (negative), 1+ (weakly positive), 2+ (moderately positive), or 3+ (strongly positive). In each case the immunoreactivity was determined in 5 random high-powered fields and the count was done independently by 2 observers.

Statistical Analysis. Categorical variables were compared using Fisher's exact test. Paired comparison of continuous data was performed using the Wilcoxon signed ranks test. To assess whether the 2 variables covary, Spearman's rank correlation coefficient was determined. Cumulative survival curves were calculated by the Kaplan-Meier method and analyzed by the log-rank test. All statistical analyses were performed using the JMP statistical software package (SAS Institute Inc., Cary, NC). A P value less than 0.05 was considered statistically significant.

Results

Clinicopathological Profiles. Forty-three patients with HCC were recruited in this study, including 27 men and 16 women, with ages ranging from 25 to 78 (median 65) years old. Clinicopathological profiles of the patients and their HCCs are shown in Table 1. Antibody to hepatitis C virus was found in sera of 72% of the patients, and hepatitis B virus surface antigen was positive in 21%.

According to the TNM staging, 60% were stage I to II and 40% were stage III to IV. In noncancerous portions of the resected livers, cirrhosis and chronic hepatitis[18] were found in 68% and 30%, respectively, of the specimens, whereas only 1 (2%) was of normal histology. Fibrocapsular formation surrounding HCC was observed in 84% and capsular invasion by HCC cells in 33%. Portal vein involvement and satellite nodules suggesting intrahepatic metastasis were found in 21% and 37%, respectively.

Detection of Gankyrin with the Monoclonal Anti-gankyrin Antibody. To determine the specificity of the monoclonal anti-gankyrin antibody 3A6C2, we expressed wild-type full-length or truncated gankyrin (Fig. 1A) in 293T cells. The antibody detected all mutants of gankyrin, suggesting that the epitope exists within the third and fifth ankyrin-repeat region (Fig. 1B). The antibody recognized the endogenous gankyrin as well, and no major cross-reacting band was observed.

Because gankyrin mRNA is known to be overexpressed in most HCCs,[9] we analyzed the levels of gankyrin protein in HCCs and surrounding noncancerous liver tissues using the 3A6C2 antibody. The protein level of gankyrin was higher in HCC tissues than in noncancerous tissues

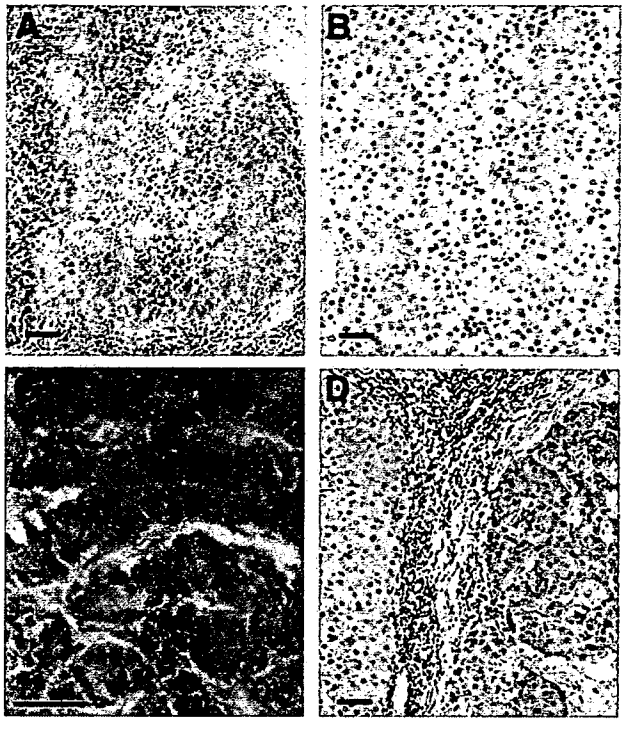

Fig. 2. Immunohistochemical detection of gankyrin in hepatocellular carcinoma (HCC). HCC sections were stained with mouse monoclonal anti-gankyrin antibody, and counterstained with hematoxylin. Positive immunostaining appears brown. (A) Positive staining for gankyrin in the cytoplasm of most HCC cells. (B) Barely detectable gankyrin signal in some HCC cells. (C) Presence of gankyrin in the nucleus of some HCC cells. (D) Stronger staining for gankyrin in HCC cells (right) than the neighboring cirrhotic hepatocytes (left). Bar, 50 μm.

(Fig. 1C). The mobilities of the gankyrin band were not different among samples.

Immunohistochemical Analysis of Gankyrin Expression. We next examined the expression of gankyrin protein in HCC and noncancerous liver tissues by immunohistochemistry. The gankyrin signal was observed mainly in the cytoplasm and occasionally in the nucleus of HCC cells (Fig. 2A-C). Although at lower levels compared with those in HCCs, weak but reproducible gankyrin signals were observed in the cytoplasm of the hepatocytes in the noncancerous tissues (Fig. 2D). Expression of gankyrin was not detected in the bile duct cells, blood endothelial cells, or other nonparenchymal cells in the liver tissues. Of 43 HCCs examined, the cytoplasm was stained positively for gankyrin in 27 (63%), and 9 of them (21%) were also positive for nuclear staining. Of 32 noncancerous liver tissues available, gankyrin was positive in 17 (53%).

As shown in Table 2, we analyzed an association between gankyrin protein expression and clinicopathological findings. No significant association between gankyrin expression in HCC cells and sex, age, tumor size, fibrotic change in noncancerous liver tissues, differentiation of the tumor cells, or hepatitis B or C virus infection was observed. Positive cytoplasmic staining for gankyrin of HCC cells was significantly associated with low TNM stage (stage I or II; $P = 0.004$), no capsular invasion ($P = 0.018$), no portal venous invasion ($P = 0.008$), and no intrahepatic metastasis ($P = 0.012$) of HCC. In noncancerous liver tissues, positive gankyrin staining of hepatocytes was associated with the cytoplasmic gankyrin positivity of HCC cells of the same patient ($P = 0.021$, Table 3), but not with the parameters examined except for the serum alpha-fetoprotein level ($P = 0.015$, Table 2).

Because expression of gankyrin affects the degradation of p53 and MDM2,[16] we examined the expression of p53 and MDM2 as well as gankyrin in HCCs. By immunohistochemistry, nuclear expression of p53 and MDM2 were detected in 30% and 23%, respectively, of 43 HCCs (Fig. 3, Table 3). Positive staining for gankyrin was not associated with the staining for p53 nor MDM2 in HCC cells.

Up-regulation of IGFBP-5 Expression by Gankyrin in HCCs. Preliminary microarray analysis of the cDNA libraries prepared from U-2 OS cells and Huh-7 cells overexpressing gankyrin suggested that IGFBP-5 mRNA was up-regulated by gankyrin (A. Umemura and J. Fujita, unpublished data). Real-time RT-PCR analysis con-

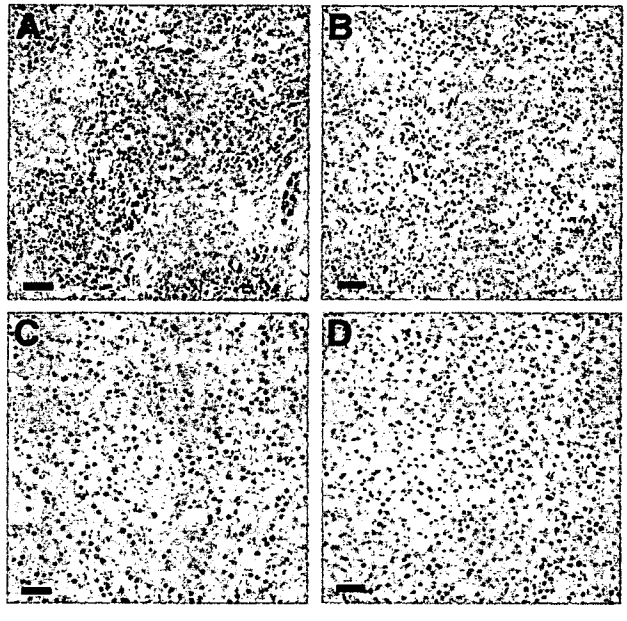

Fig. 3. Immunohistochemical detection of p53 and MDM2 in hepatocellular carcinoma (HCC). HCC sections were stained with antibodies specific to p53 (A and B) or MDM2 (C and D), and counterstained with hematoxylin. Positive immunostaining appears brown. (A) Positive staining for p53 in the nucleus of most HCC cells. (B) Negative p53 in HCC cells. (C) Positive staining for MDM2 in the nucleus of most HCC cells. (D) Negative MDM2 in HCC cells. Bar, 50 μm.

Table 2. Gankyrin Expression and Clinicopathological Characteristics

	Gankyrin Expression in the Cytoplasm of					
	HCC			Noncancerous Liver		
	Negative (n = 16)	Positive (n = 27)	*P* value	Negative (n = 15)	Positive (n = 17)	*P* value
Sex distribution						
Male	12	15	0.328	10	11	1.000
Female	4	12		5	6	
Median age (years)	64	65	0.696	63	62	0.649
Virus marker			NS			NS
HBV(+)/HCV(−)	3	3		2	2	
HBV(−)/HCV(+)	10	18		11	11	
HBV(+)/HCV(+)	1	2		2	0	
HBV(−)/HCV(−)	2	4		0	4	
Median AFP (ng/mL)	63.0	95.0	0.890	25.0	199.0	0.015
Median tumor size (cm)	4.5	4.0	0.098	4.5	4.0	0.372
Liver cirrhosis (+)	9	20	0.316	9	13	0.450
TNM stage						
I and II	5	21	0.004	8	12	0.467
III and IV	11	6		7	5	
Histological differentiation						
Well	5	7	0.737	6	3	0.243
Moderate and poor	11	20		9	14	
Capsular formation (+)	15	21	0.229	12	13	1.000
Capsular invasion (+)	9	5	0.018	4	6	0.712
Portal venous invasion (+)	7	2	0.008	4	3	0.678
Intrahepatic metastasis (+)	10	6	0.012	6	5	0.712
Gankyrin nuclear expression						
Yes	0	9	0.016	2	5	0.403
No	16	18		13	12	

Abbreviations: HCV, anti-hepatitis C virus antibody; HBV, hepatitis B surface antigen; (+), positive or present; (−), negative or absent; AFP, serum alpha-fetoprotein; NS, not significant between any groups or combinations thereof.

firmed that overexpression of gankyrin increased the IGFBP-5 mRNA levels 5.2-fold and 1.7-fold (mean, n = 3 each) in U-2 OS and Huh-7 cells, respectively, and western blot analysis demonstrated that the protein levels were increased as well (Fig. 4A). Conversely, when gankyrin expression was suppressed by siRNA, IGFBP-5 expression was down-regulated (Fig. 4B). In 2 of 3 HCC tissues overexpressing gankyrin, the levels of IGFBP-5 protein were higher compared with those in noncancerous tissues (Fig. 1C). To identify a role that IGFBP-5 might play in HCC cells, we next suppressed IGFBP-5 expression by siRNA. No apoptosis was induced, but viable cell numbers were decreased in Huh-7 as well as U-2 OS cells (Fig. 4C,D, and data not shown), suggesting a growth-promoting effect of IGFBP-5.

The expression of IGFBP-5 was further examined immunohistochemically in 43 HCC and 32 noncancerous liver tissues (Fig. 5, Table 3). In 42% of HCCs, IGFBP-5 was positively stained in the cytoplasm of HCC cells (Fig. 5A). IGFBP-5 was also detected, although at lower levels, in the cytoplasm of hepatocytes in 28% of the noncancerous tissues (Fig. 5B-D), but not in bile duct cells, blood endothelial cells, or other nonparenchymal cells.

Specific cytoplasmic staining for IGFBP-5 in HCC cells was associated with low TNM stage (stage I or II; $P = 0.013$), no portal venous invasion ($P = 0.006$), low serum alpha-fetoprotein value ($P = 0.031$), and small tumor size ($P = 0.009$). No association with capsular invasion or intrahepatic metastasis was observed. There was a significant association between positivities for IGFBP-5 and

Table 3. Gankyrin Expression and Molecular Histological Markers

	Gankyrin Expression in HCC		
	Negative	Positive	*P* value
Gankyrin expression in non-HCC			
Negative (n = 15)	8	7	0.021
Positive (n = 17)	2	15	
p53 expression in HCC			
Negative (n = 30)	11	19	1.000
Positive (n = 13)	5	8	
MDM2 expression in HCC			
Negative (n = 33)	14	19	0.276
Positive (n = 10)	2	8	
IGFBP-5 expression in HCC			
Negative (n = 25)	13	12	0.026
Positive (n = 18)	3	15	
IGFBP-5 expression in non-HCC			
Negative (n = 23)	14	9	0.011
Positive (n = 9)	1	8	

Abbreviations: HCC, hepatocellular carcinoma; non-HCC, noncancerous portion of the resected liver; IGFBP-5, insulin-like growth factor-binding protein 5.

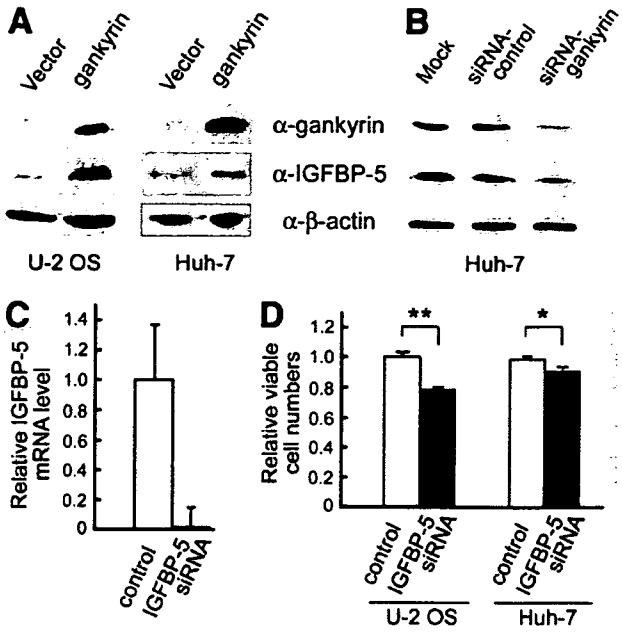

Fig. 4. Induction of IGFBP-5 by gankyrin. (A) U-2 OS cells (lanes 1 and 2) and Huh-7 cells (lanes 3 and 4) transiently transfected with plasmids expressing gankyrin or vector alone were analyzed for expression of IGFBP-5 by western blotting using the indicated antibodies. Representative results from more than 3 experiments are shown. (B) Huh-7 cells, mock transfected or transfected with siRNA for gankyrin or control RNA as indicated, were analyzed as in (A). (C) Suppression of IGFBP-5 expression by siRNA. Huh-7 cells were transfected with control RNA or IGFBP-5-specific siRNA. IGFBP-5 transcript levels were determined by real-time RT-PCR and normalized with β-actin levels. Results from 3 repeats were averaged and expressed relative to control. Error bars refer to standard deviation of the average quantitated results. (D) Effect of IGFBP-5 down-regulation on cell growth. U-2 OS and Huh-7 cells were transfected with IGFBP-5 siRNA or control RNA, and 72 hours later viable cell numbers were determined. Values are mean ± standard deviation (n = 3) and expressed relative to controls. ** and *, $P < 0.01$ and $P < 0.05$, respectively.

gankyrin (Table 3), and the levels of expression covaried both in HCCs ($\rho = 0.629$, $P < 0.001$) (Fig. 5E) and noncancerous hepatocytes ($\rho = 0.606$, $P < 0.001$) (Fig. 5F).

Expression of Gankyrin in HCC and Patient Prognosis. When we examined the relationship between gankyrin expression in HCC cells and the survival of patients after surgical resection, a significant difference was observed between the patients with gankyrin-positive HCCs and those with gankyrin-negative HCCs (Fig. 6). We found no significant difference in the survival rates between the patients whose HCCs stained positively and negatively for p53, MDM2, or IGFBP-5.

Discussion

Gankyrin is as an oncogene, mRNA of which is overexpressed in almost all human HCCs.[9,19] Although less frequent, gankyrin has been found by RNA dot blot analysis to be overexpressed in additional tumors including those of the breast, colon, rectum, stomach, small intestine, pancreas, ovary, lung, and thyroid (A. Umemura and J. Fujita, unpublished data). In the current study, we immunohistochemically examined the gankyrin protein expression in HCCs using the monoclonal anti-gankyrin antibody and found that the protein was highly expressed in the cytoplasm of 63% of HCCs. Tan et al.[20] has simi-

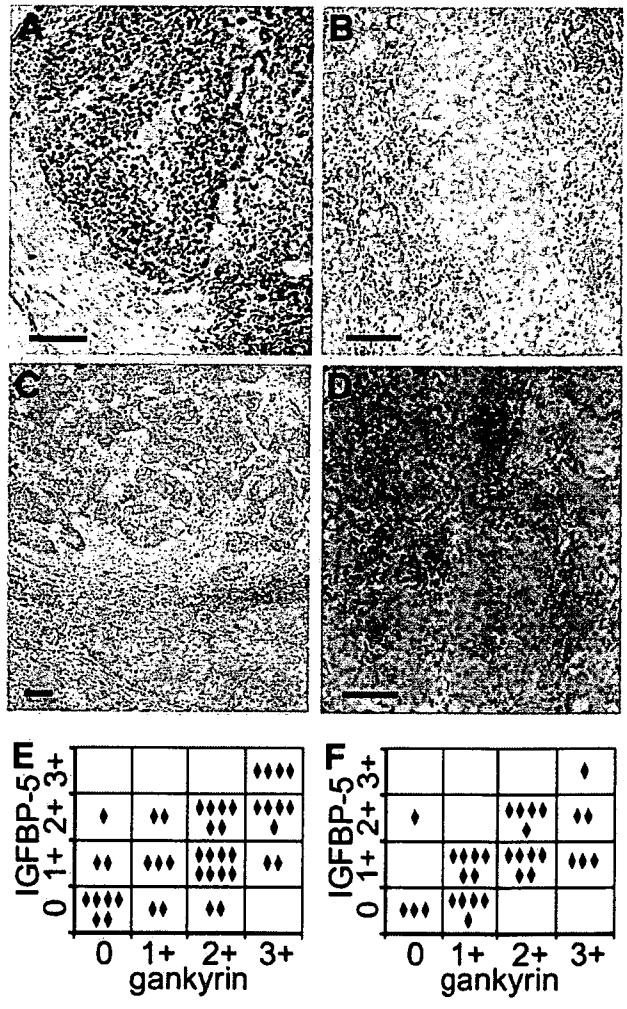

Fig. 5. Immunohistochemical detection of IGFBP-5 in hepatocellular carcinoma (HCC). HCC sections were stained with anti-IGFBP-5 antibody and counterstained with hematoxylin. Positive immunostaining appears brown. (A) Positive staining for IGFBP-5 in the cytoplasm of HCC cells, especially at the invasive boundaries. (B) Presence of IGFBP-5 in noncancerous cirrhotic hepatocytes. (C) Stronger staining for IGFBP-5 in HCC cells (upper) than the neighboring cirrhotic hepatocytes (lower). (D) Positive staining for IGFBP-5 in HCC cells (upper left), but negative in cirrhotic cells (lower right). Bar, 100 μm. (E) Correlation of expression levels of gankyrin and IGFBP-5 in HCCs. The immunostaining levels were expressed as 0 (negative), 1+ (weakly positive), 2+ (moderately positive), or 3+ (strongly positive). Each diamond represents 1 case. The Spearman's rho = 0.629, $P < 0.001$. (F) Correlation of expression levels of gankyrin and IGFBP-5 in noncancerous hepatocytes determined as in (E). The Spearman's rho = 0.606, $P < 0.001$.

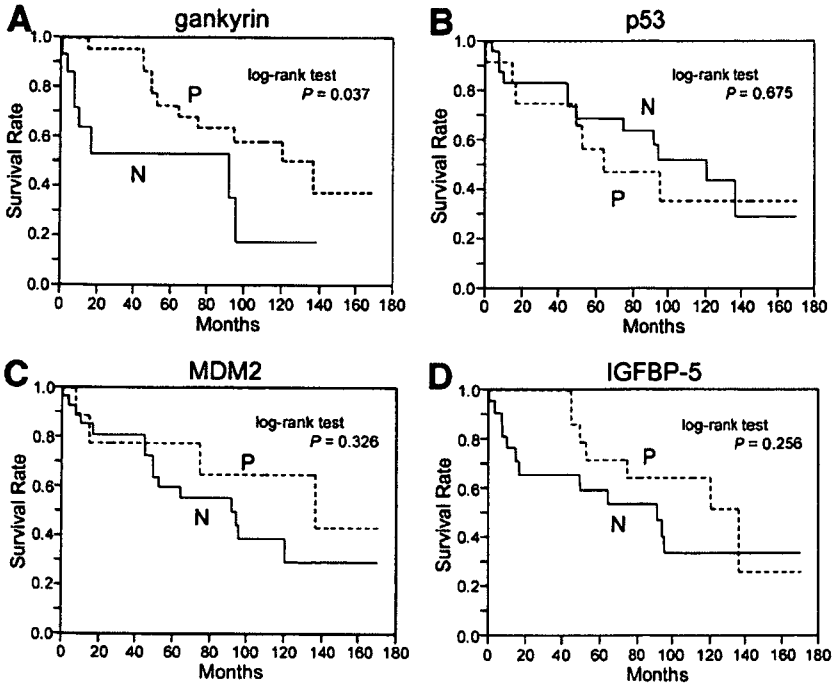

Fig. 6. Survival of patients and expression of molecular markers. The Kaplan-Meier method was used to determine the patient survival and log-rank test to compare survival between patients with HCC grouped according to (A) gankyrin positivity, (B) p53 positivity, (C) MDM2 positivity, and (D) IGFBP-5 positivity. P, positive. N, negative.

larly found overexpression of gankyrin protein in 60% of HCCs using a polyclonal antibody. The reason why the protein is not overexpressed in one-third of HCCs despite overexpression of its mRNA is unknown. The posttranscriptional, translational, and posttranslational regulations of gankyrin expression remain to be elucidated.

According to the 15th follow-up survey by the Liver Cancer Study group of Japan, the cumulative survival rates after surgical removal of HCC are 52.3% and 27.3% at 5 and 10 years, respectively, and better survival rates are associated with fewer numbers of tumors, lack of portal venous invasion, and early clinical stages.[4-6] Consistent with these observations, gankyrin positivity of HCC was associated with low TNM stage, lack of capsular invasion, portal venous invasion, and intrahepatic metastasis, and better prognosis of the patients. Patients with hyperdiploid acute lymphoblastic leukemia with more than 50 chromosomes, one of the 6 subtypes of pediatric acute lymphoblastic leukemia, have an excellent prognosis compared with other subtypes, and interestingly, overexpression of gankyrin is 1 of the diagnostic and subclassification markers for it.[21] Expression of gankyrin protein may be used as a marker for better prognosis of the patients with HCC as well.

The gankyrin oncoprotein plays a key role in regulation of cell cycle and apoptosis, at least in cultured cells, by inhibiting Rb and p53.[10] In a rodent hepatocarcinogenesis model, hypermethylation of the p16INK4A gene and p53 mutation appear at a late stage, whereas gankyrin is overexpressed from early after carcinogen treatment, preceding the loss of Rb protein and adenoma formation.[22] Clinically, p53 mutation is not so frequent in HCCs (15%-30%), especially in low-grade or low-stage HCCs.[23,24] Tan et al.[20] have immunohistochemically detected gankyrin overexpression in 82%, 63%, and 22% of Edmondson's grade I to II, III, and IV HCCs, respectively. We observed gankyrin positivity in 81% and 35% of low and high TNM stage HCCs, respectively. These results suggest that gankyrin plays an important role(s) at early stages of hepatocarcinogenesis by suppressing Rb, p53 and possibly other tumor suppressors. In advanced HCCs, by contrast, oncogenic mutations probably have accumulated in many genes including p53, and overexpression of gankyrin may not be so crucial as in early stage HCCs. This could explain the present association of gankyrin-negative HCCs with poorer prognosis and the finding that both cases of gankyrin-negative HCCs with gankyrin-positive noncancerous hepatocytes belonged to high TNM stages. This is, however, one of several possible explanations, and further work is necessary to clarify the exact reasons for the observed association.

By immunohistochemical staining, p53 has been detected in 20% to 30% of HCCs.[25, 26] Although strong immunohistochemical reactivity for p53 may not be an indicator of the presence of p53 gene mutations as initially suggested,[26] it has been associated in some studies with higher proliferative activity, lower differentiation of HCC cells, or poorer survival of patients. Endo et al.[27] immunohistochemically detected MDM2 in 28 of 107 (26%) HCCs, and the positive expression correlated with

the presence of p53 mutation and poorer prognosis, although it also correlated with smaller HCC size and the absence of vascular invasion. We immunohistochemically detected the expression of p53 and MDM2 in 30% and 23%, respectively, of HCCs, which is in accord with other studies, but no correlation was seen between expression and survival of the patients. Gankyrin accelerates degradation of Rb, p53, and MDM2 in cultured cells.[9,16] Although some correlation between expression of gankyrin and Rb has been suggested in HCC tissues,[20] we did not observe significant relationship between the gankyrin positivity and negative staining for p53 nor MDM2. The analysis of individual cells for protein expression, for example by double 2-color immunostaining, may have revealed the presence of some relationship. But most probably, our finding reflects complex interrelated mechanisms regulating the levels of these proteins and also suggests that the relevance of the effects of gankyrin on p53, MDM2, and Rb demonstrated in cultured cells to human hepatocarcinogenic process remains to be firmly established.

The 6 members of IGFBP family (IGFBP-1 through IGFBP-6) are important components of the insulin-like growth factor (IGF) axis, and regulate the activity of both IGF-I and IGF-II polypeptide growth factors.[28] IGF-I, IGF-II, and their receptors are expressed in a wide variety of cells, and the liver is the main source of circulating IGF-I. IGFBPs are also secreted by many cell types, and their expression is regulated in a cell-dependent and tissue-type–dependent manner. In the current study, we found up-regulation of IGFBP-5 mRNA and protein levels by overexpression of gankyrin in human osteosarcoma and HCC cell lines and consistently detected a significant association between the protein levels of gankyrin and IGFBP-5 in HCC specimens. In the proximal promoter region of the IGFBP-5 gene, there are several putative transcription-factor–binding sites including those for AP-2, c-Myb, C/EBP, and NF-1, and responsive elements to prostaglandin E_2, cyclic adenosine monophosphate, progesterone/retinoic acid, and Akt.[28] Whether the effect of gankyrin on IGFBP-5 expression is mediated by these factors is unknown.

The IGFBPs bind IGFs with high affinity, and they are able to enhance or inhibit the activity of IGFs in a cell-specific and tissue-type–specific manner.[28] In addition, IGFBPs have IGF-independent effects. There are several reports on the relationship between the IGF axis and HCC.[29-31] IGFBP-3 is the most abundant IGFBP present in noncancerous liver tissue and could serve as a negative regulator of cell proliferation in human HCCs.[32] Although the presence of IGFBP-5 in numerous tumors and cell lines has been demonstrated, its expression and significance in human HCC have not been documented. We found positive staining for IGFBP-5 in 42% of HCCs, and the positivity correlated with absence of portal venous invasion, low TNM stage, and small tumor size. Although not statistically significant, patients with IGFBP-5–positive HCCs tended to survive longer than those with IGFBP-5–negative HCCs. These findings are essentially similar to those observed for gankyrin. Regarding the effect of IGFBP-5 on cell proliferation, there are contradictory findings.[28] In breast cancer cells, many studies have reported inhibition of growth, but there are some indicating a stimulatory effect.[33] IGFBP-5 is up-regulated in involuting prostate but is also implicated in growth stimulation of prostate tumor cells.[34] We found that down-regulation of IGFBP-5 suppresses growth of Huh-7 HCC cells. Thus, these findings are consistent with a notion that high expression of IGFBP-5 and gankyrin play oncogenic roles in HCCs of early clinical stages. Clarification of the exact roles played by them will shed more light on the molecular mechanisms of human hepatocarcinogenesis and lead to development of new therapeutic and preventive strategies.

Acknowledgment: We thank Dr. R. John Mayer for helpful suggestions.

References

1. Parkin DM, Bray F, Ferlay J, Pisani P. Global cancer statistics, 2002. CA Cancer J Clin 2005;55:74-108.
2. Thomas MB, Zhu AX. Hepatocellular carcinoma: the need for progress. J Clin Oncol 2005;23:2892-2899.
3. Treiber G, Wex T, Rocken C, Fostitsch P, Malfertheiner P. Impact of biomarkers on disease survival and progression in patients treated with octreotide for advanced hepatocellular carcinoma. J Cancer Res Clin Oncol 2006;132:699-708.
4. Shimada K, Sano T, Sakamoto Y, Kosuge T. A long-term follow-up and management study of hepatocellular carcinoma patients surviving for 10 years or longer after curative hepatectomy. Cancer 2005;104:1939-1947.
5. Poon RT, Fan ST, Ng IO, Lo CM, Liu CL, Wong J. Different risk factors and prognosis for early and late intrahepatic recurrence after resection of hepatocellular carcinoma. Cancer 2000;89:500-507.
6. Kiyosawa K, Umemura T, Ichijo T, Matsumoto A, Yoshizawa K, Gad A, et al. Hepatocellular carcinoma: recent trends in Japan. Gastroenterology 2004;127(5 Suppl 1):S17-S26.
7. Higashitsuji H, Higashitsuji H, Nagao T, Nonoguchi K, Fujii S, Itoh K, et al. A novel protein overexpressed in hepatoma accelerates export of NF-kappa B from the nucleus and inhibits p53-dependent apoptosis. Cancer Cell 2002;2:335-346.
8. Gotoh K, Nonoguchi K, Higashitsuji H, Kaneko Y, Sakurai T, Sumitomo Y, et al. Apg-2 has a chaperone-like activity similar to Hsp110 and is overexpressed in hepatocellular carcinomas. FEBS Lett 2004;560:19-24.
9. Higashitsuji H, Itoh K, Nagao T, Dawson S, Nonoguchi K, Kido T, et al. Reduced stability of retinoblastoma protein by gankyrin, an oncogenic ankyrin-repeat protein overexpressed in hepatomas. Nat Med 2000;6:96-99.
10. Higashitsuji H, Liu Y, Mayer RJ, Fujita J. The oncoprotein gankyrin negatively regulates both p53 and RB by enhancing proteasomal degradation. Cell Cycle 2005;4:1335-1337.
11. Hori T, Kato S, Saeki M, DeMartino GN, Slaughter CA, Takeuchi J, et al. cDNA cloning and functional analysis of p28 (Nas6p) and p40.5 (Nas7p),

two novel regulatory subunits of the 26S proteasome. Gene 1998;216:113-122.
12. Dawson S, Apcher S, Mee M, Higashitsuji H, Baker R, Uhle S, et al. Gankyrin is an ankyrin-repeat oncoprotein that interacts with CDK4 kinase and the S6 ATPase of the 26 S proteasome. J Biol Chem 2002;277: 10893-10902.
13. Li J, Tsai MD. Novel insights into the INK4-CDK4/6-Rb pathway: counter action of gankyrin against INK4 proteins regulates the CDK4-mediated phosphorylation of Rb. Biochemistry 2002;41:3977-3983.
14. Shan YF, Zhou WP, Fu XY, Yan HX, Yang W, Liu SQ, et al. The role of p28GANK in rat oval cells activation and proliferation. Liver Int 2006;26: 240-247.
15. Iwai A, Marusawa H, Kiuchi T, Higashitsuji H, Tanaka K, Fujita J, et al. Role of a novel oncogenic protein, gankyrin, in hepatocyte proliferation. J Gastroenterol 2003;38:751-758.
16. Higashitsuji H, Higashitsuji H, Itoh K, Sakurai T, Nagao T, Sumitomo Y, et al. The oncoprotein gankyrin binds to MDM2/HDM2, enhancing ubiquitylation and degradation of p53. Cancer Cell 2005;8:75-87.
17. Ueno S, Tanabe G, Nuruki K, Hamanoue M, Komorizono Y, Oketani M, et al. Prognostic performance of the new classification of primary liver cancer of Japan (4th edition) for patients with hepatocellular carcinoma: a validation analysis. Hepatol Res 2002;24:395-403.
18. Desmet VJ. Histological classification of chronic hepatitis. Acta Gastroenterol Belg 1997;60:259-267.
19. Fu XY, Wang HY, Tan L, Liu SQ, Cao HF, Wu MC. Overexpression of p28/gankyrin in human hepatocellular carcinoma and its clinical significance. World J Gastroenterol 2002;8:638-643.
20. Tan L, Fu XY, Liu SQ, Li HH, Hong Y, Wu MC, et al. Expression of p28GANK and its correlation with RB in human hepatocellular carcinoma. Liver Int 2005;25:667-676.
21. Yeoh EJ, Ross ME, Shurtleff SA, Williams WK, Patel D, Mahfouz R, et al. Classification, subtype discovery, and prediction of outcome in pediatric acute lymphoblastic leukemia by gene expression profiling. Cancer Cell 2002;1:133-143.
22. Park TJ, Kim HS, Byun KH, Jang JJ, Lee YS, Lim IK. Sequential changes in hepatocarcinogenesis induced by diethylnitrosamine plus thioacetamide in Fischer 344 rats: induction of gankyrin expression in liver fibrosis, pRB degradation in cirrhosis, and methylation of p16(INK4A) exon 1 in hepatocellular carcinoma. Mol Carcinog 2001;30:138-150.
23. Tanaka S, Toh Y, Adachi E, Matsumata T, Mori R, Sugimachi K. Tumor progression in hepatocellular carcinoma may be mediated by p53 mutation. Cancer Res 1993;53:2884-2887.
24. Hayashi H, Sugio K, Matsumata T, Adachi E, Takenaka K, Sugimachi K. The clinical significance of p53 gene mutation in hepatocellular carcinomas from Japan. HEPATOLOGY 1995;22:1702-1707.
25. Nagao T, Kondo F, Sato T, Nagato Y, Kondo Y. Immunohistochemical detection of aberrant p53 expression in hepatocellular carcinoma: correlation with cell proliferative activity indices, including mitotic index and MIB-1 immunostaining. Hum Pathol 1995;26:326-333.
26. Anzola M, Saiz A, Cuevas N, Lopez-Martinez M, Martinez de Pancorbo MA, Burgos JJ, et al. High levels of p53 protein expression do not correlate with p53 mutations in hepatocellular carcinoma. J Viral Hepat 2004;11: 502-510.
27. Endo K, Ueda T, Ohta T, Terada T. Protein expression of MDM2 and its clinicopathological relationships in human hepatocellular carcinoma. Liver 2000;20:209-215.
28. Beattie J, Allan GJ, Lochrie JD, Flint DJ. Insulin-like growth factor-binding protein-5 (IGFBP-5): a critical member of the IGF axis. Biochem J 2006;395:1-19.
29. Gong Y, Cui L, Minuk GY. The expression of insulin-like growth factor binding proteins in human hepatocellular carcinoma. Mol Cell Biochem 2000;207:101-104.
30. Scharf JG, Dombrowski F, Ramadori G. The IGF axis and hepatocarcinogenesis. Mol Pathol 2001;54:138-144.
31. Breuhahn K, Longerich T, Schirmacher P. Dysregulation of growth factor signaling in human hepatocellular carcinoma. Oncogene 2006;25:3787-3800.
32. Huynh H, Chow PK, Ooi LL, Soo KC. A possible role for insulin-like growth factor-binding protein-3 autocrine/paracrine loops in controlling hepatocellular carcinoma cell proliferation. Cell Growth Differ 2002;13: 115-122.
33. McCaig C, Perks CM, Holly JM. Intrinsic actions of IGFBP-3 and IGFBP-5 on Hs578T breast cancer epithelial cells: inhibition or accentuation of attachment and survival is dependent upon the presence of fibronectin. J Cell Sci 2002;115:4293-4303.
34. Miyake H, Pollak M, Gleave ME. Castration-induced up-regulation of insulin-like growth factor binding protein-5 potentiates insulin-like growth factor-I activity and accelerates progression to androgen independence in prostate cancer models. Cancer Res 2000;60:3058-3064.

Int. J. Cancer: **122**, 2148–2153 (2008)

Synergistic antitumor activity of the novel SN-38-incorporating polymeric micelles, NK012, combined with 5-fluorouracil in a mouse model of colorectal cancer, as compared with that of irinotecan plus 5-fluorouracil

Takako Eguchi Nakajima[1,2], Masahiro Yasunaga[2], Yasuhiko Kano[3], Fumiaki Koizumi[4], Ken Kato[1], Tetsuya Hamaguchi[1], Yasuhide Yamada[1], Kuniaki Shirao[1], Yasuhiro Shimada[1] and Yasuhiro Matsumura[2]*

[1]*Gastrointestinal Oncology Division, National Cancer Center Hospital, Tokyo, Japan*
[2]*Investigative Treatment Division, Research Center for Innovative Oncology, National Cancer Center Hospital East, Kashiwa, Chiba, Japan*
[3]*Hematology Oncology, Tochigi Cancer Center, Tochigi, Japan*
[4]*Shien Lab Medical Oncology Division, National Cancer Center Hospital, Tokyo, Japan*

The authors reported in a previous study that NK012, a 7-ethyl-10-hydroxy-camptothecin (SN-38)-releasing nano-system, exhibited high antitumor activity against human colorectal cancer xenografts. This study was conducted to investigate the advantages of NK012 over irinotecan hydrochloride (CPT-11) administered in combination with 5-fluorouracil (5FU). The cytotoxic effects of NK012 or SN-38 (an active metabolite of CPT-11) administered in combination with 5FU was evaluated *in vitro* in the human colorectal cancer cell line HT-29 by the combination index method. The effects of the same drug combinations was also evaluated *in vivo* using mice bearing HT-29 and HCT-116 cells. All the drugs were administered i.v. 3 times a week; NK012 (10 mg/kg) or CPT11 (50 mg/kg) was given 24 hr before 5FU (50 mg/kg). Cell cycle analysis in the HT-29 tumors administered NK012 or CPT-11 *in vivo* was performed by flow cytometry. NK012 exerted more synergistic activity with 5FU compared to SN-38. The therapeutic effect of NK012/5FU was significantly superior to that of CPT-11/5FU against HT-29 tumors ($p = 0.0004$), whereas no significant difference in the antitumor effect against HCT-116 tumors was observed between the 2-drug combinations ($p = 0.2230$). Cell-cycle analysis showed that both NK012 and CPT-11 tend to cause accumulation of cells in the S phase, although this effect was more pronounced and maintained for a more prolonged period with NK012 than with CPT-11. Optimal therapeutic synergy was observed between NK012 and 5FU, therefore, this regimen is considered to hold promise of clinical benefit, especially for patients with colorectal cancer.

Key words: NK012; SN-38; 5-fluorouracil; drug delivery system; colorectal cancer

The 5-year survival rates of colorectal cancer (CRC) have improved remarkably over the last 10 years, accounted for in large part by the extensively investigated agents after 5-fluorouracil (5FU). Irinoetcan hydrochloride (CPT-11), a water-soluble, semi-synthetic derivative of camptothecin, is one such agent that has been shown to be highly effective, and currently represents a key-drug in first- and second-line treatment regimens for CRC. CPT-11 monotherapy, however, has not been shown to yield superior efficacy, including in terms of the median survival time, to bolus 5FU/leucovorin (LV) alone.[1] In 2 Phase III trials, the addition of CPT-11 to bolus or infusional 5FU/LV regimens clearly yielded greater efficacy than administration of 5FU/LV alone, with a doubling of the tumor response rate and prolongation of the median survival time by 2–3 months.[1,2]

CPT-11 is converted to 7-ethyl-10-hydroxy-camptothecin (SN-38), a biologically active and water-insoluble metabolite of CPT-11, by carboxylesterases in the liver and the tumor. SN-38 has been demonstrated to exhibit up to a 1,000-fold more potent cytotoxic activity than CPT-11 against various cancer cells *in vitro*.[3] The metabolic conversion rate is, however, very low, with only <10% of the original volume of CPT-11 being metabolized to SN-38[4,5]; conversion of CPT-11 to SN-38 also depends on genetic interindividual variability of the activity of carboxylesterases.[6] Direct use of SN-38 itself for clinical cancer treatment must be shown to be identical in terms of both efficacy and toxicity.

Some drugs incorporated in drug delivery systems (DDS), such as Abraxane and Doxil, are already in clinical use.[7,8] The clinical benefits of DDS are based on their EPR effect.[9] The EPR effect is based on the pathophysiological characteristics of solid tumor tissues: hypervascularity, incomplete vascular architecture, secretion of vascular permeability factors stimulating extravasation within cancer tissue, and absence of effective lymphatic drainage from the tumors that impedes the efficient clearance of macromolecules accumulated in solid tumor tissues. Several types of DDS can be used for incorporation of a drug. A liposome-based formulation of SN-38 (LE-SN38) has been developed, and a clinical trial to assess its efficacy is now under way.[10,11]

Recently, we demonstrated that NK012, novel SN-38-incorporating polymeric micelles, exerted superior antitumor activity and less toxicity than CPT-11.[12] NK012 is characterized by a smaller size of the particles than LE-SN38; the mean particle diameter of NK012 is 20 nm. NK012 can release SN-38 under neutral conditions even in the absence of a hydrolytic enzyme, because the bond between SN-38 and the block copolymer is a phenol ester bond, which is stable under acidic conditions and labile under mild alkaline conditions. The release rate of SN-38 from NK012 under physiological conditions is quite high; more than 70% of SN-38 is released within 48 hr. We speculated that the use of NK012, in place of CPT-11, in combination with 5FU may yield superior results in the treatment of CRC. In the present study, we evaluated the antitumor activity of NK012 administered in combination with 5FU as compared to that of CPT-11 administered in combination with 5FU against CRC in an experimental model.

Material and methods

Cells and animals

The human colorectal cancer cell lines used, namely, HT-29 and HCT-116, were purchased from the American Type Culture Collection (Rockville, MD). The HT-29 cells and HCT-116 cells were maintained in RPMI 1640 supplemented with 10% fetal bovine serum (Cell Culture Technologies, Gaggenau-Hoerden, Germany), penicillin, streptomycin, and amphotericin B (100 units/mL, 100 μg/mL, and 25 μg/mL, respectively; Sigma, St. Louis, MO) in a humidified atmosphere containing 5% CO_2 at 37°C.

BALB/c *nu/nu* mice were purchased from SLC Japan (Shizuoka, Japan). Six-week-old mice were subcutaneously (s.c.)

***Correspondence to:** Investigative Treatment Division, Research Center for Innovative Oncology, National Cancer Center Hospital East, 6-5-1 Kashiwanoha, Kashiwa, Chiba 277-8577, Japan. Fax: +81-4-7134-6866.
E-mail: yhmatsum@east.ncc.go.jp
Received 2 September 2007; Accepted after revision 20 November 2007
DOI 10.1002/ijc.23381
Published online 14 January 2008 in Wiley InterScience (www.interscience.wiley.com).

inoculated with 1×10^6 cells of HT-29 or HCT-116 cell line in the flank region. The length (a) and width (b) of the tumor masses were measured twice a week, and the tumor volume (TV) was calculated as follows: $TV = (a \times b^2)/2$. All animal procedures were performed in compliance with the Guidelines for the Care and Use of Experimental Animals established by the Committee for Animal Experimentation of the National Cancer Center; these guidelines meet the ethical standards required by law and also comply with the guidelines for the use of experimental animals in Japan.

Drugs

The SN-38-incorporating polymeric micelles, NK012, and SN-38 were prepared by Nippon Kayaku (Tokyo, Japan).[12] CPT-11 was purchased from Yakult Honsha (Tokyo, Japan). 5FU was purchased from Kyowa Hakko (Tokyo, Japan).

Cell growth inhibition assay

HT-29 cells were seeded in 96-well plates at a density of 2,000 cells/well in a final volume of 90 μL. Twenty-four hours after seeding, a graded concentration of NK012 or SN-38 was added concurrently with 5FU to the culture medium of the HT-29 cells in a final volume of 100 μL for drug interaction studies. The culture was maintained in the CO_2 incubator for an additional 72 hr. Then, cell growth inhibition was measured by the tetrazolium salt-based proliferation assay (WST assay; Wako Chemicals, Osaka, Japan). WST-1 labeling solution (10 μL) was added to each well and the plates were incubated at 37°C for 3 hr. The absorbance of the formazan product formed was detected at 450 nm in a 96-well spectrophotometric plate reader. Cell viability was measured and compared to that of the control cells. Each experiment was carried out in triplicate and was repeated at least 3 times. Data were averaged and normalized against the nontreated controls to generate dose-response curves.

Drug interaction analysis

The nature of interaction between NK012 or SN-38 and 5FU against HT-29 cells was evaluated by median-effect plot analyses and the combination index (CI) method of Chou and Talalay.[13] Data analysis was performed using the Calcusyn software (Biosoft, NY, USA). NK012 or SN-38 was combined with 5FU at a fixed ratio that spanned the individual IC_{50} values of each drug. The IC_{50} values were determined on the basis of the dose-response curves using the WST assay. For any given drug combination, the CI is known to represent the degree of synergy, additivity or antagonism. It is expressed in terms of fraction-affected (Fa) values, which represents the percentage of cells killed or inhibited by the drug. Isobologram equations and Fa/CI plots were constructed by computer analysis of the data generated from the median effect analysis. Each experiment was performed in triplicate with 6 gradations and was repeated at least 3 times. The resultant dose-response curves were averaged, to create a single composite dose-response curve for each combination.

In vivo analysis of the effects of NK012 combined with 5FU as compared to those of CPT-11 combined with 5FU

When the mean tumor volumes reached ~93 mm^3, the mice were randomly divided into test groups consisting of 5 mice per group (Day 0). The drugs were administered i.v. *via* the tail vein of the mice. In the groups administered NK012 or 5FU as single agents, the drug was administered on Days 0, 7 and 14. In the combined treatment groups, NK012 or CPT-11 was administered 24 hr before 5FU on Days 0, 7 and 14, according to the previously reported combination schedule for CPT-11 and 5FU.[14] Complete response (CR) was defined as tumor not detectable by palpation at 90 days after the start of treatment, at which time-point the mice were sacrificed. Tumor volume and body weight were measured twice a week. As a general rule, animals in which the tumor volume exceeded 2,000 mm^3 were also sacrificed.

Experiment 1. Evaluation of the effects of NK012 combined with 5FU and determination of the maximum tolerated dose (MTD) of NK012/5FU. By comparing the data between NK012 administered as a single agent and NK012/5FU, we evaluated the effects of the combined regimen against the s.c HT-29 tumors. A preliminary experiment showed that combined administration of NK012 15 mg/kg + 5FU 50 mg/kg every 6 days caused drug-related lethality (data not shown). To determine the MTD, therefore, we set the dosing schedule of the combined regimen at 5 or 10 mg/kg of NK012 + 50 mg/kg of 5FU three times a week.

Experiment 2. Comparison of the antitumor effect of NK012/5FU and CPT-11/5FU. Based on a comparison of the data between NK012/5FU and CPT-11/5FU against the s.c. HT-29 and HCT-116 tumors, we investigated the feasibility of the clinical application of NK012/5FU for the treatment of CRC. CPT-11/5FU was administered three times a week at the respective MTDs of the 2 drugs as previously reported, that is, CPT11 at 50 mg/kg and 5FU at 50 mg/kg, respectively.[14] NK012/5FU was administered once three times a week at the respective MTDs of the 2 drugs determined from Experiment 1.

Cell cycle analysis

Samples from the HT-29 tumors that had grown to 80–100 mm^3 were removed from the mice at 6, 24, 48, 72 and 96 hr after the administration of NK012 alone at 10 mg/kg or CPT-11 alone at 50 mg/kg. The samples were excised, minced in PBS and fixed in 70% ethanol at −20°C for 48 hr. They were then digested with 0.04% pepsin (Sigma chemical Co., St Lous, MO) in 0.1 N HCL for 60 min at 37°C in a shaking bath to prepare single-nuclei suspensions. The nuclei were then centrifuged, washed twice with PBS and stained with 40 μg/mL of propidium iodide (Molecular Probes, OR) in the presence of 100 μg/mL RNase in 1 mL PBS for 30 min at 37°C. The stained nuclei were analyzed with B-D FACSCalibur (BD Biosciences, San Jose, CA), and the cell cycle distribution was analyzed using the Modfit program (Verity Software House Topsham, ME).

Statistical analyses

Data were expressed as mean ± SD. Data were analysed with Student's t test when the groups showed equal variances (F test), or Welch's test when they showed unequal variances (F test). $p < 0.05$ was regarded as statistically significant. All statistical tests were 2-sided.

Results

Antiproliferative effects of NK012 or SN-38 administered in combination with 5FU

Figure 1*a* shows the dose-response curves for NK012 alone, 5FU alone and a combination of the two. The IC_{50} levels of NK012 and 5FU against the HT-29 cells were 39 nM and 1 μM, respectively, and the IC_{50} level of SN-38 was 14 nM (data not shown). Based on these data, the molar ratio of NK012 or SN-38:5FU of 1:1,000 was used for the drug combination studies.

Figures 1*b* and 1*c* show the median-effect and the combination index plots. Combination indices (CIs) of <1.0 are indicative of synergistic interactions between 2 agents; additive interactions are indicated by CIs of 1.0, and antagonism by CIs of >1.0. Figure 1*c* shows the combination index for NK012 and 5FU, when 2 drugs are supposed to be mutually exclusive. Marked synergism was observed between Fa 0.2 and 0.6. Theoretically, the CI method is the most reliable around an Fa of 0.5, suggesting synergistic effects of the combination of NK012 and 5FU. This synergistic effect was more evident than that of SN-38/5FU (Fig. 1*d*).

In vivo *effect of combined NK012 and 5FU*

Experiment 1. Dose optimization and effect of combined NK012 and 5FU against HT-29 tumors. Comparison of the relative tumor volumes on Day 40 revealed significant differences between

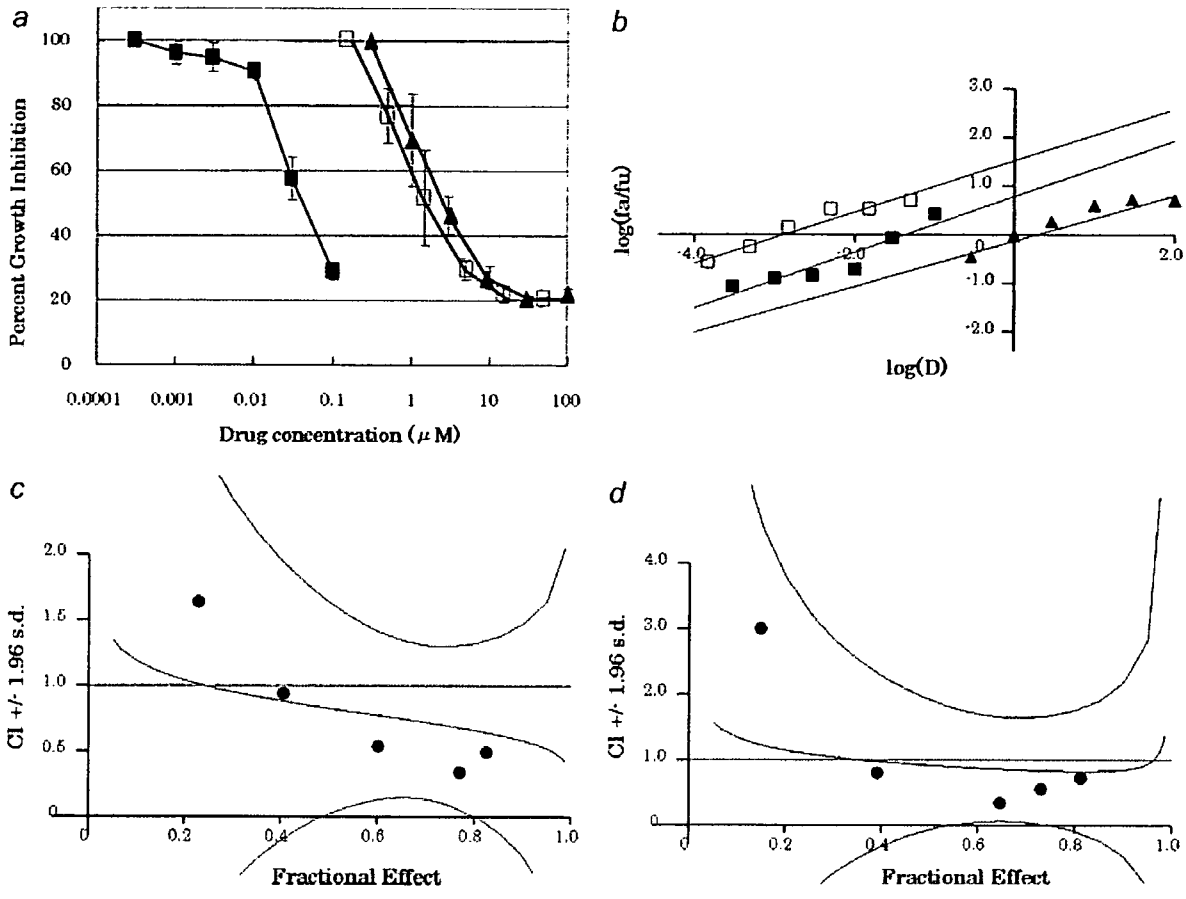

FIGURE 1 – Interaction of NK012 and 5FU *in vitro*. (*a*) Dose-response curves for NK012 alone (■), 5FU alone (▲) and their combination (□) against HT-29 cells. HT-29 cells were seeded at 2,000 cells/well. Twenty-four hours after seeding, a graded concentration of NK012 or 5FU was added to the culture medium of the HT-29 cells. Cell growth inhibition was measured by WST assay after 72 hr of treatment. Cell viability was measured and compared with that of the control cells. Each experiment was carried out independently and repeated at least 3 times. Points, mean of tripricates; bars, SD. (*b*) Median effect plot for the interaction of NK012 and 5FU. (*c*, *d*) Combination index for the interaction as a function of the level of effect (fraction effect = 0.5 is the IC_{50}). The straight line across the CI value of 1.0 indicates additive effect and CIs above and below indicate antagonism and synergism, respectively. The molar ratio of NK012/5FU (*c*) or SN-38/5FU (*d*) at 1:1,000 was tested by CI analysis. Black circles represent the CIs of the actual data points, solid lines represent the computer-derived CIs at effect levels ranging from 10 to 100% inhibition of cell growth, and the dotted lines represent the 95% confidence intervals.

those in the mice administered NK012 alone and those administered NK012/5FU at 5 mg/kg of NK012 ($p = 0.018$) (Fig. 2*a*). Although there was no statistically significant difference in the relative tumor volume measured on Day 54 between the mice administered NK012 alone and NK012/5FU at 10 mg/kg of NK012 ($p = 0.3050$), a trend of superior antitumor effect was demonstrated in the group treated with NK012/5FU at 10 mg/kg of NK012 (Fig. 2*a*). The CR rates were 20, 40 and 60% for 5 mg/kg NK012 + 50 mg/kg 5FU, 10 mg/kg NK012 alone and 10 mg/kg NK012 + 50 mg/kg 5FU, respectively. The schedule of 10 mg/kg NK012 + 50 mg/kg 5FU resulted in no remarkable toxicity in terms of body weight changes, and these doses were determined as representing the MTDs (Fig. 2*b*).

Experiment 2. Comparison of the antitumor effect of combined NK012/5FU and CPT-11/5FU against HT-29 and HCT-116 tumors. The therapeutic effect of NK012/5FU on Day 60 was significantly superior to that of CPT-11/5FU against the HT-29 tumors ($p = 0.0004$) (Fig. 3*a*). A more potent antitumor effect, namely, a 100% CR rate, was obtained in the NK012/5FU group as compared to the 0% CR rate in the CPT-11/5FU group. Although no statistically significant difference in the relative tumor volume on Day 61 was demonstrated between the NK012/5FU and CPT-11/5FU in the case of the HCT-116 tumors ($p = 0.2230$), a trend of superior antitumor effect against these tumors was observed in the NK012/5FU treatment group (Fig. 3*b*). The CR rates for the case of the HCT-116 tumors were 0% in both NK012/5FU and CPT-11/5FU groups.

Specificity of cell cycle perturbation

We studied the differences in the effects between NK012 10 mg/kg and CPT-11 50 mg/kg on the cell cycle (Fig. 4*a*). The data indicated that both NK012 and CPT-11 tended to cause accumulation of cells in the S phase, although the effect of NK012 was stronger and maintained for a more prolonged period than that of CPT-11; the maximal percentage of S-phase cells in the total cell population in the tumors was 34% at 24 hr after the administration of CPT-11, whereas it was 39% at 48 hr after the administration of NK012 (Figs. 4*b*, and 4*c*).

Discussion

Our primary endpoint was to clarify the advantages of NK012 over CPT-11 administered in combination with 5FU. We demonstrated that combined NK012 and 5FU chemotherapy exerts more

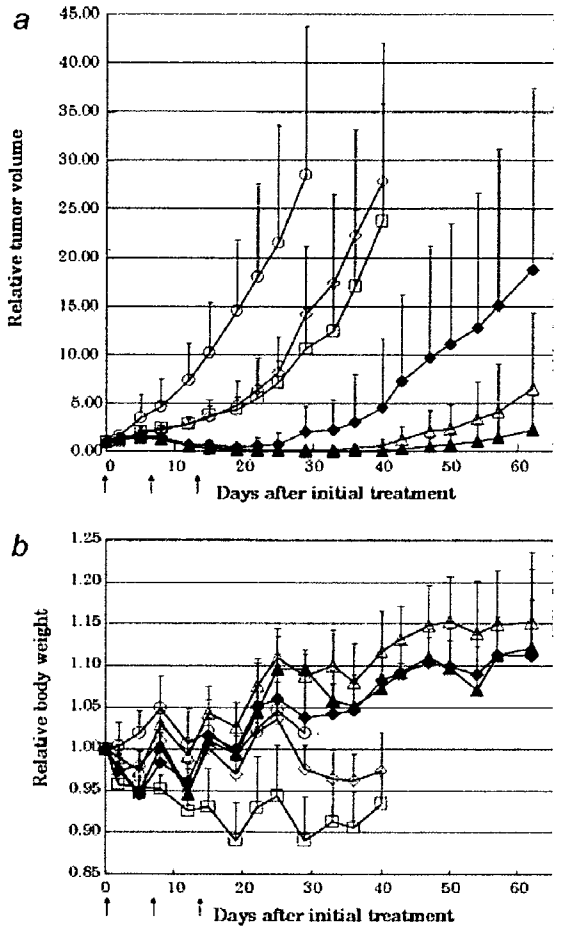

FIGURE 2 – Effect of NK012 alone or NK012 in combination with 5FU against HT-29 tumor-bearing mice. Points, mean; bars, SD. (*a*) Antitumor effect of each regimen on Days 0, 7 and 14. (○) control, (□) 5FU 50 mg/kg alone, (◇) NK012 5 mg/kg alone, (◆) NK012 5 mg/kg 24 hr before 5FU 50 mg/kg, (△) NK012 10 mg/kg alone, (▲) NK012 10 mg/kg 24 hr before 5FU 50 mg/kg. (*b*) Changes in the relative body weight. Data were derived from the same mice as those used in the present study.

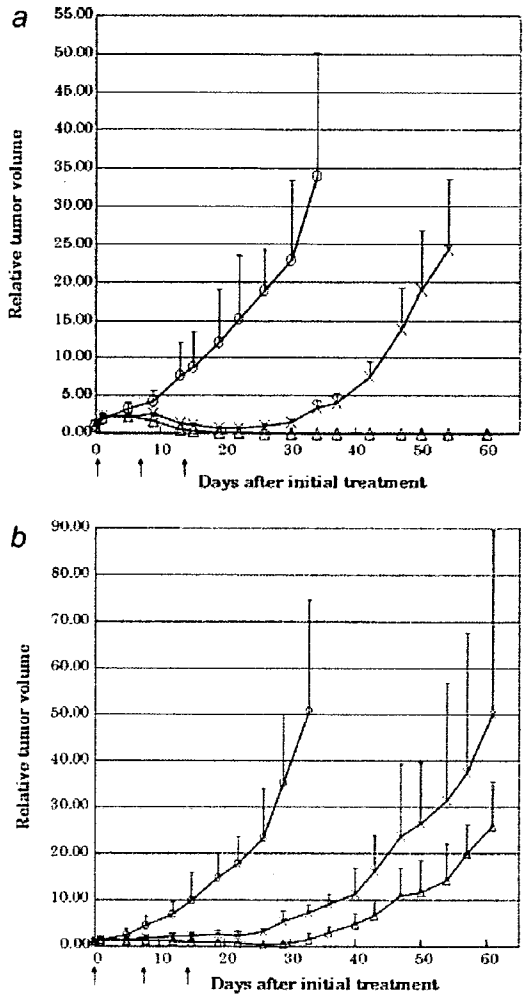

FIGURE 3 – Effect of NK012/5FU as compared with that of CPT11/5FU against HT-29 (*a*) or HCT-116 (*b*) tumor-bearing mice. Antitumor effect of each schedule on Days 0, 7 and 14. (○) control, (×) CPT-11 50 mg/kg 24 hr before 5FU 50 mg/kg, (△) NK012 10 mg/kg 24 hr before 5FU 50 mg/kg. Points, mean; bars, SD.

synergistic activity *in vitro* and significantly greater antitumor activity against human CRC xenografts as compared to CPT-11/5FU. The combination of NK012 and 5FU is considered to hold promise of clinical benefit for patients with CRC.

CPT-11, a topoisomerase-I inhibitor, and 5FU, a thymidilate synthase inhibitor, have been demonstrated to be effective agents for the treatment of CRC. A combination of these 2 drugs has also been demonstrated to be clearly more effective than either CPT-11 or 5FU/LV administered alone *in vivo* and in clinical settings.[1,2,14] Administration of 5FU by infusion with CPT-11 was shown to be associated with reduced toxicity and an apparent improvement in survival as compared to that of administration of the drug by bolus injection with CPT-11.[1,2] This synergistic enhancement may result from the mechanism of action of the 2 drugs; CPT-11 has been reported to cause accumulation of cells in the S phase, and 5FU infusion is known to cause DNA damage specifically in cells of the S phase.[14] On the basis of this background, our results suggesting the more pronounced and more prolonged accumulation of the tumor cells in the S phase caused by NK012 as compared with that by CPT-11 may explain the more effective synergy of the former administered with 5FU infusion. This may be attributable to accumulation of NK012 due to the enhanced permeability and retention (EPR) effect.[9] It is also speculated that NK012 allows sustained release of free SN-38, which may move more freely in the tumor interstitium.[15] Otherwise NK012 itself could internalize into cells to localize in several cytoplasmic organelles as reported by Savic *et al.*[16] These characteristics of NK012 may be responsible for its more potent antitumor activity observed in this study, because CPT-11 has been reported to show time-dependent growth-inhibitory activity against the tumor cells.[17]

The major dose-limiting toxicities of CPT-11 are diarrhea and neutropenia. SN-38, the active metabolite of CPT-11, may cause CPT-11-related diarrhea as a result of mitotic -inhibitory activity.[18] Because it undergoes significant biliary excretion, SN-38 may have a potentially long residence time in the gastrointestinal tract that may be associated with prolonged diarrhea.[19,20] In our previous report, we evaluated the tissue distribution of SN-38 after administration of an equimolar amount of NK012 (20 mg/kg) and CPT-11 (30 mg/kg), and found no difference in the level of SN-38 accumulation in the small intestine.[12] A significant antitumor effect of NK012 with a lower incidence of diarrhea was also dem-

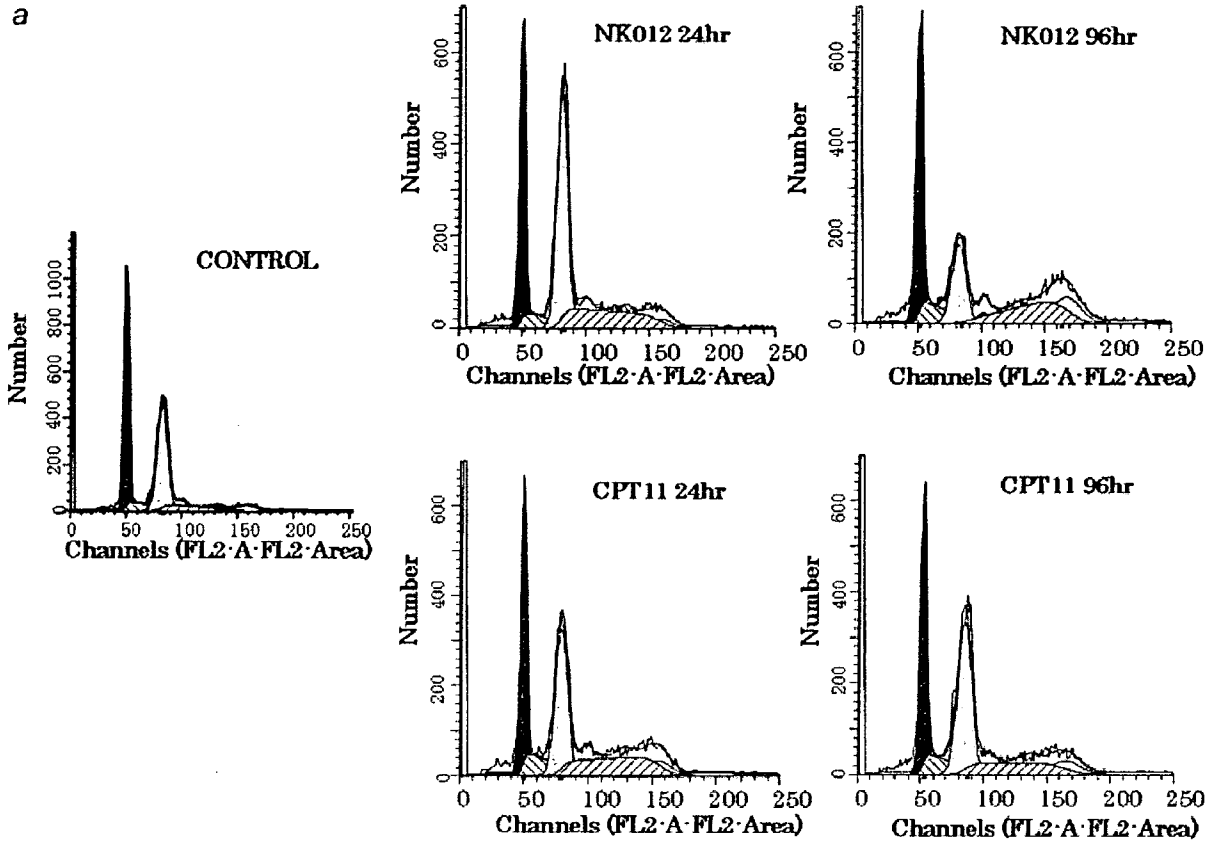

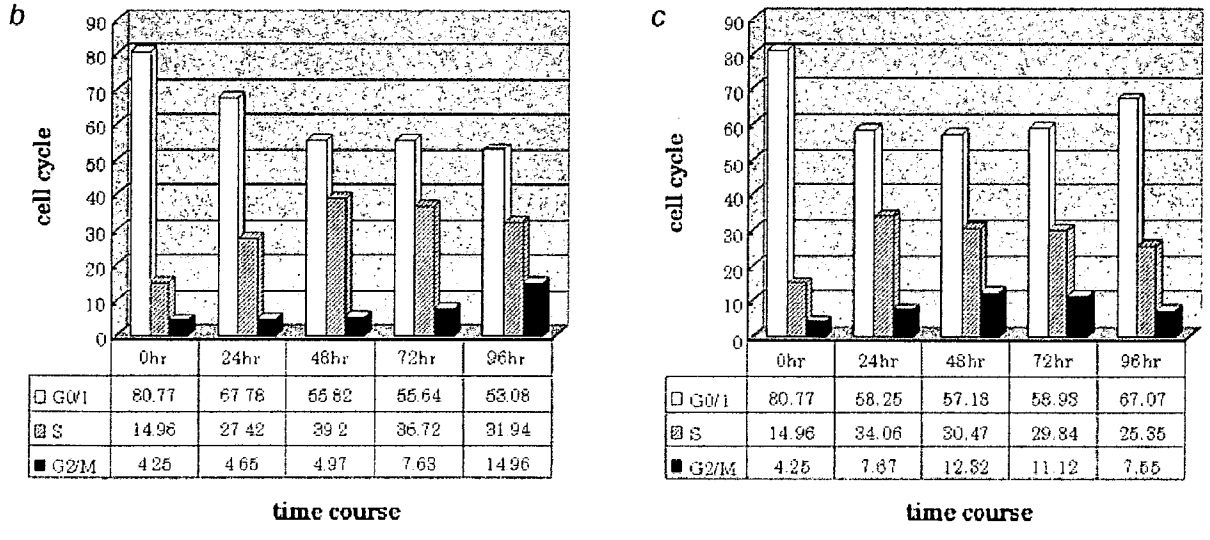

b	0hr	24hr	48hr	72hr	96hr
G0/1	80.77	67.76	55.82	55.64	53.08
S	14.96	27.42	39.2	36.72	31.94
G2/M	4.25	4.65	4.97	7.63	14.96

c	0hr	24hr	48hr	72hr	96hr
G0/1	80.77	58.25	57.18	58.98	67.07
S	14.96	34.06	30.47	29.84	25.35
G2/M	4.25	7.67	12.32	11.12	7.55

FIGURE 4 – Cell cycle analysis of HT-29 tumor cells collected 24, 48, 72 and 96 hr after administration of NK012 at 10 mg/kg alone or CPT-11 at 50 mg/kg alone using the Modfit program (Verity Software House Topsham, ME). (*a*) Cell cycle analysis of HT-29 tumor cells 24 and 96 hr after administration of NK012 at 10 mg/kg or CPT-11 at 50 mg/kg, respectively. (*b*) Cell cycle distribution of tumor cells 0, 24, 48, 72 and 96 hr after treatment with NK012 at 10 mg/kg. (*c*) Cell cycle distribution of tumor cells 0, 24, 48, 72 and 96 hr after treatment with CPT-11 at 50 mg/kg.

onstrated as compared to that observed with CPT-11 in a rat mammary tumor model.[21] Combined administration of CPT-11 with 5FU/LV infusion appears to be associated with acceptable toxicity in patients with CRC. In addition, no significant difference in the frequency of Grade 3/4 diarrhea was noted between patients treated with FOLFIRI (CPT-11 regimen with bolus and infusional 5FU/LV) and those treated with FOLFOX6 (oxaliplatin regimen with bolus and infusional 5FU/LV).[22,23] Our *in vivo* data actually revealed no severe body weight loss in the NK012/5FU group. Consequently, we expect that the NK012/5FU regimen, especially

with infusional 5FU, may be an attractive arm for a Phase III trial in CRC, with CPT-11/5FU as the control arm. We have already initiated a Phase I trial of NK012 in patients with advanced solid tumors based on the data suggesting higher efficacy and lower toxicity of this preparation than CPT-11 *in vivo*.[12]

In conclusion, we demonstrated that combined NK012 and 5FU chemotherapy exerts significantly greater antitumor activity against human CRC xenografts as compared to CPT-11/5FU, indicating the necessity of clinical evaluation of this combined regimen.

References

1. Saltz LB, Douillard JY, Pirotta N, Alakl M, Gruia G, Awad L, Elfring GL, Locker PK, Miller LL. Irinotecan plus fluorouracil/leucovorin for metastatic colorectal cancer: a new survival standard. Oncologist 2001;6:81–91.
2. Douillard JY, Cunningham D, Roth AD, Navarro M, James RD, Karasek P, Jandik P, Iveson T, Carmichael J, Alakl M, Gruia G, Awad L, et al. Irinotecan combined with fluorouracil compared with fluorouracil alone as first-line treatment for metastatic colorectal cancer: a multicentre randomised trial. Lancet 2000;355:1041–7.
3. Takimoto CH, Arbuck SG. Topoisomerase I targeting agents: the camptothecins. In: Chabner BA, Lango DL, eds. Cancer chemotherapy and biotherapy: principal and practice, 3rd ed. Philadelphia, PA: Lippincott Williams and Wilkins, 2001. 579–646.
4. Slatter JG, Schaaf LJ, Sams JP, Feenstra KL, Johnson MG, Bombardt PA, Cathcart KS, Verburg MT, Pearson LK, Compton LD, Miller LL, Baker DS, et al. Pharmacokinetics, metabolism, and excretion of irinotecan (CPT-11) following I.V. infusion of [(14)C]CPT-11 in cancer patients. Drug Metab Dispos 2000;28:423–33.
5. Rothenberg ML, Kuhn JG, Burris HA, III, Nelson J, Eckardt JR, Tristan-Morales M, Hilsenbeck SG, Weiss GR, Smith LS, Rodriguez GI, Rock MK, Von Hoff DD. Phase I and pharmacokinetic trial of weekly CPT-11. J Clin Oncol 1993;11:2194–204.
6. Guichard S, Terret C, Hennebelle I, Lochon I, Chevreau P, Fretigny E, Selves J, Chatelut E, Bugat R, Canal P. CPT-11 converting carboxylesterase and topoisomerase activities in tumour and normal colon and liver tissues. Br J Cancer 1999;80:364–70.
7. Gradishar WJ, Tjulandin S, Davidson N, Shaw H, Desai N, Bhar P, Hawkins M, O'Shaughnessy J. Phase III trial of nanoparticle albumin-bound paclitaxel compared with polyethylated castor oil-based paclitaxel in women with breast cancer. J Clin Oncol 2005;23:7794–803.
8. Muggia FM. Liposomal encapsulated anthracyclines: new therapeutic horizons. Curr Oncol Rep 2001;3:156–62.
9. Matsumura Y, Maeda H. A new concept for macromolecular therapeutics in cancer chemotherapy: mechanism of tumoritropic accumulation of proteins and the antitumor agent smancs. Cancer Res 1986;46:6387–92.
10. Zhang JA, Xuan T, Parmar M, Ma L, Ugwu S, Ali S, Ahmad I. Development and characterization of a novel liposome-based formulation of SN-38. Int J Pharm 2004;270:93–107.
11. Kraut EH, Fishman MN, LoRusso PM, Gorden MS, Rubin EH, Haas A, Fetterly GJ, Cullinan P, Dul JL, Steinberg JL. Final result of a phase I study of liposome encapsulated SN-38 (LE-SN38): safety, pharmacogenomics, pharmacokinetics, and tumor response [abstract 2017]. Proc Am Soc Clin Oncol 2005;23:139S.
12. Koizumi F, Kitagawa M, Negishi T, Onda T, Matsumoto S, Hamaguchi T, Matsumura Y. Novel SN-38-incorporating polymeric micelles, NK012, eradicate vascular endothelial growth factor-secreting bulky tumors. Cancer Res 2006;66:10048–56.
13. Chou TC, Talalay P. Quantitative analysis of dose-effect relationships: the combined effects of multiple drugs or enzyme inhibitors. Adv Enzyme Regul 1984;22:27–55.
14. Azrak RG, Cao S, Slocum HK, Toth K, Durrani FA, Yin MB, Pendyala L, Zhang W, McLeod HL, Rustum YM. Therapeutic synergy between irinotecan and 5-fluorouracil against human tumor xenografts. Clin Cancer Res 2004;10:1121–9.
15. Jain RK. Barriers to drug delivery in solid tumors. Sci Am 1994; 271:58–65.
16. Savic R, Luo L, Eisenberg A, Maysinger D. Micellar nanocontainers distribute to defined cytoplasmic organelles. Science 2003;300:615–18.
17. Kawato Y, Aonuma M, Hirota Y, Kuga H, Sato K. Intracellular roles of SN-38, a metabolite of the camptothecin derivative CPT-11, in the antitumor effect of CPT-11. Cancer Res 1991;51:4187–91.
18. Slater R, Radstone D, Matthews L, McDaid J, Majeed A. Hepatic resection for colorectal liver metastasis after downstaging with irinotecan improves survival. Proc Am Soc Clin Oncol 2003;22(abstract 1287).
19. Araki E, Ishikawa M, Iigo M, Koide T, Itabashi M, Hoshi A. Relationship between development of diarrhea and the concentration of SN-38, an active metabolite of CPT-11, in the intestine and the blood plasma of athymic mice following intraperitoneal administration of CPT-11. Jpn J Cancer Res 1993;84:697–702.
20. Atsumi R, Suzuki W, Hakusui H. Identification of the metabolites of irinotecan, a new derivative of camptothecin, in rat bile and its biliary excretion. Xenobiotica 1991;21:1159–69.
21. Onda T, Nakamura I, Seno C, Matsumoto S, Kitagawa M, Okamoto K, Nishikawa K, Suzuki M. Superior antitumor activity of NK012, 7-ethyl-10-hydroxycamptoyhecin-incorporating micellar nanoparticle, to irrinotecan. Proc Am Assoc Cancer Res 2006;47:720s(abstract 3062).
22. Tournigand C, Andre T, Achille E, Lledo G, Flesh M, Mery-Mignard D, Quinaux E, Couteau C, Buyse M, Ganem G, Landi B, Colin P, et al. FOLFIRI followed by FOLFOX6 or the reverse sequence in advanced colorectal cancer: a randomized GERCOR study. J Clin Oncol 2004;22:229–37.
23. Colucci G, Gebbia V, Paoletti G, Giuliani F, Caruso M, Gebbia N, Carteni G, Agostara B, Pezzella G, Manzione L, Borsellino N, Misino A, et al. Phase III randomized trial of FOLFIRI versus FOLFOX4 in the treatment of advanced colorectal cancer: a multicenter study of the Gruppo Oncologico Dell'Italia Meridionale. J Clin Oncol 2005; 23:4866–75.

Expression profiling of fecal colonocytes for RNA-based screening of colorectal cancer

SATOSHI YAJIMA[1,2], MIE ISHII[3], HISAYUKI MATSUSHITA[4], KAZUHIKO AOYAGI[1], KAZUHIKO YOSHIMATSU[5], HIRONORI KANEKO[2], NOBUKO YAMAMOTO[3], TATSUO TERAMOTO[2], TERUHIKO YOSHIDA[1], YASUHIRO MATSUMURA[4] and HIROKI SASAKI[1]

[1]Genetics Division, National Cancer Center Research Institute, Tsukiji 5-1-1, Chuo-ku, Tokyo 104-0045; [2]Division of General and Gastroenterological Surgery (Omori), Department of Surgery, School of Medicine, Faculty of Medicine, Toho University, Omori Nishi 6-11-1, Ohta-ku, Tokyo 143-8541; [3]Medical Engineering Development Center, Canon Inc., Shimomaruko 3-30-2, Ohta-ku, Tokyo 146-8501; [4]Investigate Treatment Division, Research Center for Innovative Oncology, National Cancer Center Hospital East, Kashiwanoha 6-5-1, Kashiwa, Chiba 277-8577; [5]Medical Center East, Tokyo Women's Medical University, School of Medicine, Nishiogu 2-1-10, Arakawa-ku, Tokyo 116-8567, Japan

Received May 21, 2007; Accepted July 18, 2007

Abstract. The early detection of colorectal cancer originating from any part of the colorectum is desirable because this cancer can be cured surgically if diagnosed early. We searched for marker genes for a fecal RNA-based colorectal cancer screening method by comparison of genome-wide expression profiles among cancerous and non-cancerous tissues, and healthy volunteer- and cancer patient-derived colonocytes from the feces, and the peripheral blood. Of 14,564 genes, only 3 (PAP, REG1A, and DPEP1) were selectable as final candidates which were expressed frequently at any stage of this cancer and were suppressed in non-cancerous tissues and also in the peripheral blood and colonocytes of healthy volunteers. Next, we directly compared fecal RNA-expression profiles between colorectal cancer patients and healthy volunteers, and found that most of the genes (92%) expressed in the colonocytes of the cancer patients were not expressed in those of the healthy volunteers. Six genes (SEPP1, RPL27A, ATP1B1, EEF1A1, SFN, and RPS11) selected randomly from 85 cancer patient-derived colonocyte-specific genes were evaluated. In total, reverse transcription-polymerase chain reaction or focused microarray of all those 9 genes detected 18 (78%) of 23 curable colorectal cancers (Dukes stages A-C), 9 or 10 (64% or 71%) of 14 early cancers with no lymph node metastasis (Dukes stage A or B) and 4 (80%) of 5 right-sided cancers. Our extensive gene list provides other markers for fecal RNA-based colorectal cancer screening.

Correspondence to: Dr Hiroki Sasaki, Genetics Division, National Cancer Center Research Institute, Tsukiji 5-1-1, Chuo-ku, Tokyo 104-0045, Japan
E-mail: hksasaki@gan2.res.ncc.go.jp

Key words: expression profiling, colonocyte, colorectal cancer screening, microarray

Introduction

Colorectal cancer is a common malignancy which is curable by surgical resection if diagnosed at a sufficiently early stage (stage I/Dukes stage A or stage II/Dukes stage B). Five-year survival rates on surgical resection, for example, at Dukes stage A, Dukes stage B and stage III/Dukes stage C are 95%, 80% and 50-60%, respectively. For stage IV/Dukes stage D, curative resection is impossible. Therefore, early detection of this cancer originating from any part of the colorectum is desired. For mass cancer screenings, a simple, economic, and noninvasive method of cancer detection is required. The Hemoccult test is currently used in many countries for this purpose (1-5). However, this test is nonspecific and is not sufficiently sensitive to detect early-stage cancer, although a higher sensitivity has been reported for the advanced stage (6).

For fecal DNA-based colorectal cancer screening, in 1992, Sidransky first reported Ras oncogene mutations in the fecal DNA of patients with curable colorectal cancer (7). To date, many screening methods based on mutated DNA detection in the feces have been reported (8-19). These methods, however, are time-consuming and are not sufficiently sensitive. The major reason for this inaccuracy is the fact that fecal DNAs are derived from an enormous number and variety of bacteria and normal living cells including normal colorectal mucus cells, lymphocytes, red blood cells and anal squamous cells. Immunocytochemical analysis provides a simple method; however, this method is insensitive because only the surface portion of the feces can be assayed. On the other hand, Tarin and colleagues first reported that cancer-specific CD44 splicing variants are useful for fecal RNA-based colorectal cancer screening (20,21). By the use of the repetition of the Percoll centrifugation method for isolating the colonocytes from feces, we have also demonstrated that unusual CD44 variants could be targets for cancer-detection using feces (22). However, the method is found to distort the morphology of